Open access • Journal Article • DOI:10.1016/J.PALAEO.2013.02.032

Modern foraminifera, δ13C, and bulk geochemistry of central Oregon tidal marshes and their application in paleoseismology — Source link

Simon E. Engelhart, Simon E. Engelhart, B. Horton, B. Horton ...+5 more authors

Institutions: University of Rhode Island, University of Pennsylvania, Rutgers University, British Geological Survey ...+3 more institutions

Published on: 01 May 2013 - Palaeogeography, Palaeoclimatology, Palaeoecology (Elsevier)

Topics: Low marsh, High marsh and Foraminifera

Published in Paleo3, (2013) 377,13-27

Modern salt-marsh foraminifera, flora and stable carbon isotopes of Siletz Bay, Oregon, and their application in paleoseismology

Simon E. Engelhart[1,2*], Benjamin P. Horton[1], Christopher H. Vane[3], Alan R. Nelson[4], Robert C. Witter[5], Sarah R. Brody[6], and Andrea D. Hawkes[7].

1. Sea Level Research, Department of Earth and Environmental Science, University of Pennsylvania, Hayden Hall, 240 South 33rd St, Philadelphia, PA, 19104, USA
2. Department of Geosciences, University of Rhode Island, Woodward Hall, 9 East Alumni Avenue, Kingston, RI, 02881, USA
3. British Geological Survey, Kingsley Dunham Centre, Keyworth, Nottingham, NG12 5GG, UK
4. Geological Hazards Team, US Geological Survey, MS 966, P.O. Box 25046, Denver, CO, 80225, USA
5. Alaska Science Center, US Geological Survey, 4200 University Drive, Anchorage, AK, 99508, USA
6. Nicholas School of the Environment, Duke University, Box 90328, Durham, NC, 27708, USA
7. Geology and Geophysics Department, Woods Hole Oceanographic Institution, Woods Hole, MA, 02543, USA

*Corresponding Author: simoneng@sas.upenn.edu (+1 215 898 7889)

Published in Paleo3, (2013) 377,13-27

Abstract

We compared foraminifera, flora and geochemical ($\delta^{13}C$, total organic content and C:N) analyses to reconstruct the magnitude of coastal subsidence during the AD1700 great megathrust earthquakes at the Cascadia subduction zone. Four modern transects collected from three intertidal zones at Siletz Bay, Oregon, USA, produced three elevation dependent groups in both the foraminifera and geochemical datasets. Foraminiferal samples from the tidal flat and low marsh are identified by *M. fusca* abundances of > 45%, middle and high marsh by *M. fusca* abundances of < 45% and highest marsh by *T. irregularis* abundances > 25%. The $\delta^{13}C$ values from the geochemically defined groups decrease with increasing elevation; -24.1 ± 1.7‰ in the tidal flat and low marsh; -27.3 ± 1.4‰ in the middle and high marsh; and -29.6 ± 0.8‰ in the highest marsh samples. We applied these modern foraminfera and geochemical distributions to a core that contained the AD 1700 earthquake. Both techniques produced similar results for the coseismic subsidence (0.88 ± 0.39m and 0.71 ± 0.56m) suggesting that $\delta^{13}C$ has potential as a efficient proxy for use in paleoseismology.

1. Introduction

To evaluate and prepare for the impacts of future great earthquakes along the Cascadia subduction zone of North America, it is necessary to understand the magnitude and recurrence interval of previous earthquakes over geological timescales (Atwater, 1987; Charland and Priest, 1995; Clague, 1997; Wang and

Clark, 1999; Peterson et al., 2000; Frankel et al., 2002; Kelsey et al., 2002; Petersen et al., 2002; Priest et al., 2010). Estuaries along Cascadia coasts archive stratigraphic evidence of great earthquakes (M 8-9) during the Holocene as records of abrupt relative sea-level (RSL) changes (Darienzo and Peterson, 1995; Nelson et al., 1996b; Shennan et al., 1998; Clague et al., 2000; Kelsey et al., 2002; Witter et al., 2003; Atwater et al., 2005; Nelson et al., 2006). Microfossil-based reconstructions have the potential to produced precise estimates of coseismic subsidence (Guilbault et al., 1995; Hemphill-Haley, 1995; Nelson et al., 1996a; Sherrod, 1999; Hughes et al., 2002; Nelson et al., 2008; Hawkes et al., 2011), because of the relationship between species distributions and elevation with respect to the tidal frame (Horton and Edwards, 2006).

Salt-marsh foraminifera have been commonly utilized to reconstruct changes in RSL in tectonically quiescent areas in Europe (Horton, 1999; Gehrels et al., 2001; Horton and Edwards, 2005; Edwards, 2006) and eastern North America (Scott and Medioli, 1978; Gehrels et al., 2002; Gehrels et al., 2004; Leorri et al., 2006; Horton et al., 2009; Kemp et al., 2009b; Kemp et al., 2011; Wright et al., 2011). Quantitative foraminiferal-based reconstructions such as transfer functions (Kemp et al., 2011) have a precision of less than ± 0.1 m, which has led to similar applications in tectonic areas such as Cascadia (Guilbault et al., 1995; Guilbault et al., 1996; Nelson et al., 2008; Hawkes et al., 2010; Hawkes et al., 2011). Despite the obvious advantages, this technique is prone to problems associated with the site-specific nature of the assemblages (Wright et al., 2011) that necessitates the collection of multiple local datasets (e.g., Horton and Edwards, 2006; Kemp et al., 2011).

Stable carbon isotope analyses ($\delta^{13}C$, total organic carbon (TOC), Carbon to Nitrogen ratios (C:N) potentially provides the means to produce an alternative proxy for the reconstruction of past RSL changes (Tornqvist et al., 2004; Gonzalez and Tornqvist, 2009; Kemp et al., 2010; Kemp et al., 2012). Its utility is derived from the assumption that bulk sediment stable carbon isotope values should reflect the botanical origin (Chmura and Aharon, 1995; Lamb et al., 2006; Gonzalez and Tornqvist, 2009; Kemp et al., 2010). Similar to foraminifera, plant species communities with different isotopic signatures are controlled by the strong elevational and environmental gradient found along the transition from freshwater to salt marsh and sub-tidal environments (Chmura et al., 1987; Goni and Thomas, 2000). The application of stable carbon isotopes in bulk sediments in sea-level reconstructions is in its infancy, including studies in the UK (Lloyd and Evans, 2002; Wilson et al., 2005; Lamb et al., 2007; Mackie et al., 2007), US Atlantic (Kemp et al., 2010; Kemp et al., 2012) and US Gulf (Tornqvist et al., 2004; Gonzalez and Tornqvist, 2009) coasts.

In this study, we investigated the modern distributions of foraminifera, flora and geochemistry from three salt marshes in Siletz Bay, Oregon that have differing salinity regimes. We defined elevation dependent ecological zones of foraminifera and compared them with $\delta^{13}C$, TOC and C:N to offer a method to reconstruct former sea levels, which we applied to a record of the AD 1700 earthquake at Siletz Bay.

2. Study Area

Siletz Bay is an estuarine system separated from the Pacific Ocean by Salishan spit (Figure 1B). The bay formed when the river valley was drowned by rising RSL during the Holocene transgression (Bottom et al., 1979; Peterson et al., 1984). The Bay drains an area of 524 km^2 (Seliskar and Gallagher, 1983) and contained 1.07 – 1.46 km^2 of salt marsh in the early 1970s (Eilers, 1975; Jefferson, 1975), with an additional 0.4 km^2 reclaimed from previously dyked pastureland by the Siletz Bay National Wildlife Refuge in 2003. The Siletz River produces spatially variable salinity within the estuary with highest values near the inlet to the Pacific Ocean in the northwest of the Bay (Gallagher and Kibby, 1980). Salinity peaks from August to October with minimum values from January to March, associated with seasonal variations in flow (Oglesby, 1968). Salinity from open water measurements taken in July from surface waters in front of each site were recorded with values of 22 at Salishan Spit, 16 at Siletz East, and 11 at Millport Slough.

Siletz Bay has a mixed semidiurnal and diurnal tidal cycle with a tidal range (mean lowest low water (MLLW) to mean highest high water (MHHW) of 2.64 m (Hawkes et al., 2010). Short term tide gauges installed in the bay at Siletz Keys and upriver in Millport Slough indicated that there was less than 7 cm difference in mean high water (MHW) and MHHW elevations relative to North American Vertical Datum (NAVD) 88(Brophy et al., 2011).

13 species of vascular plants were found in Siletz Bay in zones ranging from tidal flat, to salt marsh and terrestrial environments (Figure 2; Table 1). Dominant vegetation types included salt marsh species such as *Gaultheria* spp., *Potentilla palustris, Juncus* spp., *Agrostis* spp., *Salicornia virginica*, *Distichlis spicata*, *Scirpus* spp., *Carex lyngbyei* and *Zostera nana* and terrestrial taxa such as *Picea* spp. and *Conium maculatum*.

3. Methods

We collected samples from four modern intertidal transects. We established two transects at Salishan Spit (SS (A to A') and SS2 (B to B')) that were 115 and 146 m long respectively and 3 km from the Pacific Ocean inlet (Figure 1B and 1C). A 123 m transect 1.2 km inland of Salishan spit was established at Siletz East (D to D'), west of Route 101 (Figure 1B and 1D). The forth transect was 95 m long at Millport Slough (E to E'), 1.8 km inland of Siletz East (Figure 1B and 1E). Stations were positioned along an elevational gradient to capture the full range of environments. Salt marsh plants at each sampling station were identified from lists of common species found in Pacific Northwest tidal marshes (Seliskar and Gallagher, 1983). We ascertained the elevation of each sample using a total station, which was tied to a local benchmark. The height of the local benchmark was obtained using real time kinematic (RTK) satellite navigation and reported relative to NAVD88. Elevations were converted to MSL to enable the use of site-specific tidal predictions (e.g. mean high water, MHW) generated for every 3 km of the Oregon coastline (Hawkes et al., 2010).

We collected a sample of 10 cm^3 of surface sediment (0-1 cm) at each station for foraminiferal analysis. The effects of infaunal foraminifera in Oregon marshes has been shown to be minimal with the highest concentration of living specimens in the top 1 cm and no live specimens found at depths greater than 5 cm (Hawkes, 2008; Hawkes et al., 2010). Samples were treated with buffered ethanol after collection and stained in the field using Rose Bengal to allow differentiation of live and dead specimens. Only the dead foraminiferal data used in the analysis as they most accurately reflect the subsurface assemblages (Murray, 1982; Horton, 1999; Culver and Horton, 2005). Each sample was divided in the laboratory using sieves to isolate the 63-500 μm fraction. The greater than 500 μm fraction was checked for large foraminifera. We counted the foraminifera using a binocular microscope from a known proportion until greater than 200 dead individuals were counted, or until the entire sample had been used. Our taxonomy follows Hawkes et al. (2001) with *Ammobaculites* spp. was identified as a single taxon.

We collected an additional 5cm^3 of surface sediment at each station geochemical analyses. Samples were prepared for $\delta^{13}C$ and total organic carbon and nitrogen following REFS. The samples were washed with 5% hydrochloric acid for 24 hours before rinsing with deionised water, then dried at 45°C and ground to a fine powder using a mortar and pestle. $\delta^{13}C$ values were obtained using a Costech Elemental Analyzer, coupled on-line to an Optima dual-inlet mass spectrometer. The values were calibrated to the Vienna Pee Dee Belemnite (VPDB) scale using cellulose standard Sigma Chemical C-6413 that was included within the runs. Sample %C and %N were calculated on the same instrument with C:N ratios calibrated through an acetanilide standard and presented on a weight-to-weight basis. Replicate measurements on well-mixed samples were never different by greater than 0.2‰.

To describe the distribution of foraminifera and geochemistry ($\delta^{13}C$, TOC, C:N), we used Partitioning Around Medoids (PAM) method (Kaufman and Rousseeuw, 1990; Kemp et al., In Press) and the 'cluster' package in the computer program R (Maechler et al., 2005). The most appropriate number of zones is identified by the highest average silhouette width of all zones. We ran the analysis for all four individual transects as well as a combined dataset; one foraminiferal and geochemical transect is shown as an example with the remaining transects in the appendix. For the foraminiferal data all analysis used percentages with no cutoff value for taxa inclusion (Kemp et al., In Press).

Published in Paleo3, (2013) 377,13-27

4. Results

4.1 Modern foraminiferal, floral, and stable carbon isotope distributions

4.1.1 Salishan Spit Transect 1 (SS)

At Salishan Spit transect 1 (A-A', Figure 1C), 12 species were identified in 24 samples (Figure 2; Figure 3). The four highest elevation samples (SS-24 to SS-21) associated with highest marsh floral environments of *Gaultheria* spp. and *Juncus* spp. mixed with *Picea* spp. and ferns (Table 1) were dominated by *Trochamminita irregularis* (> 65%). This zone was associated with low $\delta^{13}C$ values (-29 to -29.5‰), high TOC (12.2 to 28.8%) with C:N ratios from 14.3 to 16.9 (Figure 4). The high marsh of *Agrostis* spp., *Juncus* spp., *S. virginica* and *D. spicata* (SS-20 to SS-15) was characterized by *Trochammina inflata* (36 to 54%) and *Haplophragmoides manilaensis* (12 to 18%). $\delta^{13}C$ values were greater than the highest marsh (-25.7 to -28.4‰), with reduced TOC (8.4 to 18.6%) but similar C:N values (11.8 to 13.7).

The *S. virginica* and *D. spicata* middle marsh (SS-14 to SS-10) recorded a switch in the dominance from *T. inflata* (37 to 0%) to *M. fusca* (22 to 99%) with decreasing elevation. The elevation of the middle marsh ranged from 1.14 to 0.67 m MSL. The input of C_4 material from *D. spicata* may be evident in the $\delta^{13}C$ values (-23.6 to -26.2‰), with a further fall in TOC (4.9 to 12.4%) but similar C:N values (10.6 to 13.7) compared to the high marsh. The low marsh, vegetated by *Scirpus* spp. (SS-9 to SS-5) was characterized by near-monospecific *Milliammina fusca* assemblage (89 to 99%). $\delta^{13}C$ values continue to increase with further marine influence (-21.1 to -24.2‰), associated with a fall in TOC (0.3 to 1.5%) and C:N (1.7 to 8.7) . The *Z. nana* tidal flat (SS-4 to SS-1) was also dominated by *M. fusca* (83 to 89%) but with the addition of *Reophax* spp. (5 to 10%). Despite the presence of the C_4 *Z. nana*, $\delta^{13}C$ values are similar to the low marsh (-23.2 to -23.6‰). TOC (1.0 to 1.4%) and C:N ratios (9.0 to 9.4) are also comparable to the low marsh.

PAM identified three foraminiferal groups (Figure 3): Group SS-Ia (average silhouette width 0.81) is dominated by *T. irregularis*; Group SS-Ib (average silhouette width 0.70) is identified by *T. inflate* and Group SS-II (average silhouette width 0.80) is dominated by *M. fusca.* PAM identified two geochemical groups. Group SS-G-I had an average silhouette width of 0.53 with $\delta^{13}C$ value of -27.5 ± 1.4‰, TOC of 14.5 ± 5.6% and C:N of 13.3 ± 1.5. Group SS-G-II (average silhouette width 0.73) is associated with $\delta^{13}C$ values of -23.2 ± 1.1‰, TOC of 1.7 ±1.5% and C:N of 8.4 ± 2.5. Group SS-G-I is associated with *T. inflata* and *T. irregularis* whilst SS-G-II is dominated by *M. fusca*.

4.1.2 Salishan Spit Transect 2 (SS2)

At Salishan Spit transect 2 (B-B'; Figure 1C), 14 species were identified in 27 samples (Figure 2; Supplementary Figure 1). The three highest elevation samples (SS2-1 to SS2-3) taken in the transition between highest marsh communities (*P. palustris* and *Gaultheria* spp.) and terrestrial environments (*C. maculatum* and ferns) did not contain any foraminifera. The $\delta^{13}C$ are -27.5 to -28.4‰ with TOC ranging from 34.6 to 39.6% and C:N ratios of 21.0 to 29.2 (Figure 4). The highest sample with foraminifera (SS2-4) was dominated by *T. irregularis* (59%) with a low concentration (790 per $10 cm^3$) and associated with *Juncus* spp. vegetation. The *Agrostis* spp., *S. virginica*, *Juncus* spp., *D. spicata* and *P. palustris* vegetated high marsh (SS2-4 to SS2-13) was dominated by *T. inflata* (maximum 66%) with contributions from *Jadammina macrescens* (maximum 23%) and *H. wilberti* (maximum 35%). $\delta^{13}C$ values in this zone ranged from -28.5 to -24.8‰ and are associated with high TOC (9.1 to 29.9%) and C:N (11.6 to 19.2) values.

The middle marsh (SS2-14 to SS2-18) was vegetated by *D. spicata* and *S. virginica* and associated with increasing *M. fusca* (2 to 64%) and decreasing *T. inflata* (4 to 60%) over an elevation range from 0.83 to 1.15 m MSL. $\delta^{13}C$ values were lower than the high marsh (-21.3 to -24.6‰), with an associated decrease in TOC (3.6 to 7.1%) but similar C:N ratios (10.2 to 17.2). This vegetation zone is associated with increasing *M. fusca* and decreasing *T. inflata* abundances (0.83 to 1.15 m MSL). The *Scirpus* spp. low marsh (SS2-19 to SS2-22) is dominated by *M. fusca* (68 to 92%). $\delta^{13}C$ values are similar to the middle marsh (-22.2 to -23.6‰) but with a decrease in TOC (0.7 to 2.1%) and C:N ratios (8.5 to 9.6) The *Z. nana* vegetated tidal flat samples (SS2-23 to SS2-27) are also dominated by *M. fusca* (79 to 92%) with the addition of *Reophax* spp. (1-6%). $\delta^{13}C$ values are similar to the low marsh (-23.1 to -24.2‰). TOC values remain stable (0.8 to 1.9%) as do C:N ratios (8.8 to 9.9).

PAM identified two foraminiferal groups (Supplementary Figure 1): Group SS2-I had an average silhouette width of 0.51 and was dominated by *T. inflate*; and Group SS2-II (average silhouette width 0.79) is identified by high abundances of *M. fusca*. PAM also identified two geochemical groups. Group SS2-G-I had an average silhouette width of 0.74 with $\delta^{13}C$ value of -28.0 ± 0.5‰, TOC of 35.5 ± 4.2% and C:N of 25.5 ± 4.4. Group SS2-G-II (average silhouette width 0.71) is associated with $\delta^{13}C$ values of -24.3 ± 2.0‰, TOC of 6.2 ± 5.9% and C:N of 11.8 ± 2.8. Group SS2-G-1 is associated with samples absent of foraminifera or dominated by *T. irregularis* whilst SS2-G-II is dominated by *T. inflata* and *M. fusca*.

4.1.3 Siletz East Transect (SE)

At Siletz East (C-C'; Figure 1D), 11 species were identified in 17 samples (Figure 2; Supplementary Figure 2). The highest marsh vegetation identified at the Salishan Spit transects was absent at Siletz East. The *Agrostis* spp., *Juncus* spp. and *D. spicata* high marsh zone (SE1 to SE3) was characterized by *T. inflata* (4 to 30%), *J. macrescens* (16 to 54%), *Balticammina pseudomacrescens* (3 to 28%) and *H. wilberti* (8 to 53%). $\delta^{13}C$ values are consistent with input from C_3 vegetation (-25.2 to -26.9‰). TOC (2.1 to 5.6%) and C:N ratios (10.6 to 14.0) are similar to the bordering low marsh (Figure 4). The middle marsh vegetation zone seen at Salishan Spit is absent at Siletz East. The low marsh dominated by *C. lyngbyei* (SE4 to SE8) is associated with increasing *M. fusca* abundances (54 to 97%) with decreasing elevation (from 0.91 to 0.67 m MSL). $\delta^{13}C$ are lower than the high marsh (-23.8 to -28.1‰), with a fall in TOC (1.8 to 6.3%) and C:N ratios (8.4 to 14.0) with decreasing elevation. The unvegetated tidal flat (SE9 to SE17) was almost monospecific *M. fusca* (82 to 97%). $\delta^{13}C$ were greater than the low marsh (-22.3 to -25.4‰), a trend also seen in TOC (1.4 to 2.9%) and C:N ratios (7.9 to 11.6).

PAM identified two foraminiferal groups (Supplementary Figure 2): Group SE-I (average silhouette width 0.46) is composed of *T. inflata*, *J. macrescens*, *B. pseudomacrescens*, and *H. wilberti*; Group SE-II (average silhouette width 0.87) is dominated by *M. fusca*. Similarly, PAM identified two geochemical groups. Group SE-G-I had an average silhouette width of 0.70 with $\delta^{13}C$ values of -27.7 ± 0.7‰, TOC of 5.4 ± 1.0% and C:N of 13.9 ± 0.2. Group SE-G-II (average silhouette width 0.63) is associated with $\delta^{13}C$ values of -24.9 ± 1.1‰, TOC of 2.2 ± 0.7% and C:N of 10.2 ± 1.0. Group SE-G-I is associated with *J. macrescens*, *B. pseudomacrescens* and *H. wilberti* whilst SE-G-II is dominated by *M. fusca* and *T. inflata*.

4.1.4 Millport Slough Transect (MS)

At Millport Slough (D-D'; Figure 1E), 11 species were identified in 11 samples (Figure 2; Supplementary Figure 3). Sample MS-4, the highest elevation sample on the transect (1.39 m MSL) associated with *C. maculatum* did not contain foraminifera. The *Picea* spp. swamp (MS-11 to MS-10) was associated with a mixed assemblage of *T. irregularis* (26 to 38%), *H. wilberti* (2 to 27%), *B. pseudomacrescens* (14 to 16%) and *J. macrescens* (14 to 31%). $\delta^{13}C$ values were low (-29.1 to -29.6‰) with high TOC (29.6 to 31.0%) and C:N ratios (20.7 to 21.9) (Figure 4). The high marsh was vegetated by *P. palustris*, *Triglochin maritima* and *Juncus* spp. (MS-9 to MS-5) and characterized by increased abundances of *T. irregularis* (30 to 61%), *M. petilla* (0 to 18%), *H. manilaensis* (3 to 24%), *H. wilberti* (2 to 35%), and *B. pseudomacrescens* (1 to 24%). $\delta^{13}C$ was greater than in the *Picea* spp. swamp (-29.6

to -30.8‰) but with decreasing TOC (13.4 to 39.0%) and C:N ratios (14.1 to 28.0). The elevation ranged from 1.27 to 1.30 m MSL. Middle marsh vegetation is absent at this site. The *C. lyngbyei* low marsh (MS1 to MS3) is dominated by *M. fusca* (46 to 93%) with *J. macrescens* (5 to 20%) and *H. wilberti* (1 to 17%). $\delta^{13}C$ are lower relative to the *Picea* spp. swamp and high marsh (-27.5 to -28.1‰), a trend also seen in the lower TOC values (5.4 to 6.4%) and C:N ratios (13.2 to 15.3).

PAM identified two foraminiferal groups (Supplementary Figure 3): Group MS-I (average silhouette width 0.61) is dominated by *T. irregularis*; and Group MS-II (average silhouette width 0.57) is composed primarily of *M. fusca*. PAM also identified two geochemical groups. Group MS-G-I had an average silhouette width of 0.61 with $\delta^{13}C$ value of -29.9 ± 0.6‰, TOC of 30.2 ± 5.5% and C:N of 21.4 ± 4.0. Group MS-G-II (average silhouette width = 0.70) is associated with $\delta^{13}C$ values of -28.8 ± 1.1‰, TOC of 9.9 ± 4.7% and C:N of 14.5 ± 0.7. Group MS-G-I is associated with *T. irregularis*, *B. pseudomacrescens* and *H. wilberti* whilst MS-G-II is dominated by *M. fusca, J. macrescens, H. wilberti* and *T. irregularis*.

4.1.5 Combined Siletz Bay Dataset

We recorded 14 taxa (12 agglutinated and 2 calcareous) in the dead assemblage of 79 samples from four modern surface transects at three sites in Siletz Bay. Foraminifera were absent in four samples, all of which occurred at greater than 1.39 m MSL in areas of upland vegetation. The assemblages are dominated by agglutinated species including *B. pseudomacrescens*, *H. manilaensis*, *H. wilberti*, *J. macrescens*, *M. fusca*, *T. inflata* and *T. irregularis* (Table 1).

PAM identified three foraminiferal groups in the combined Siletz Bay dataset (Figure 5). Group SB-Ia (average silhouette width 0.44) is dominated by *T. irregularis* (Figure 5D). This foraminiferal assemblage is associated with highest high marsh environments at Salishan Spit transects 1 and 2 and the high marsh and *Picea* spp. swamp environments at Millport Slough. Group SB-Ib (average silhouette width 0.47) is dominated by *T. inflata* with *H. wilberti* and *J. macrescens* present in all samples. This foraminiferal group is associated with high and middle marsh vegetation. Group SB-II has the highest average silhouette width of 0.82 and is dominated by *M. fusca* and occurred at all sites.

We recorded $\delta^{13}C$, TOC and C:N for 71 samples of bulk sediment (Figure 4). All $\delta^{13}C$ measurements were less than -21.0‰ (range of -21.1 to -30.8‰). As expected, TOC was lowest in tidal flat environments and increased in vegetated environments (range of 0.3 to 39.0%). C:N values ranged from 1.7 to 28.0.

PAM identified three groups in the geochemistry of the combined Siletz Bay dataset (Figure 6). Group SB-G-I (average silhouette width = 0.64) is associated with $\delta^{13}C$ of -29.6 ± 0.8‰, TOC of 30.0 ± 4.6% and C:N of 20.4 ± 3.7. Group SB-G-II (average silhouette width = 0.45) has $\delta^{13}C$ of -27.3 ± 1.4‰, TOC of 12.4 ± 4.0% and C:N of

13.6 ± 1.4. Group SB-G-III (average silhouette width = 0.60) is characterized by $\delta^{13}C$ of -24.1 ± 1.7‰, TOC of 2.5 ± 1.8% and C:N of 10.4 ± 2.7.

5. Discussion

5.1 Modern distribution of foraminifera in Siletz Bay

We have used PAM to quantitatively sub-divide 79 modern samples of foraminifera from Siletz Bay into three faunal groups, which reflect the highest high marsh (SB-Ia), high and middle marsh (SB-Ib) and low marsh and tidal-flat (SB-II) environments. Previous studies of foraminifera along the Cascadia coastline (Figure 7) have presented similar foraminiferal assemblages (Jennings and Nelson, 1992; Guilbault et al., 1996; Hawkes et al., 2010) though there are some noticeable site-specific differences.

Group SB-Ia represents the foraminiferal assemblages found at the highest elevations in salt marshes and into the upland transition. The group elevational range extends from 1.18 to 1.60 m MSL (1.36 ± 0.15 m). This zone is dominated by *T. irregularis* (> 25%). This species has previously been identified as occupying the high marsh and upland floral zones at Salmon River, South Slough and Coquille River in Oregon (Hawkes et al., 2010) and Tofino, British Columbia (Guilbault et al., 1996). *Trochamminita spp*. including *T. irregularis* and *T. salsa* appear to be endemic to the Pacific salt marshes having been found in South America (Jennings et al., 1995) and Australasia (Hayward and Hollis, 1994; Callard et al., 2011) as well as Cascadia (Jennings and Nelson, 1992; Guilbault et al., 1996; Nelson et al., 2008;

Hawkes et al., 2010), but not along the US Atlantic coast (Gehrels, 1994) or in Europe (Horton and Edwards, 2006). *H. wilberti* is also found sporadically in group SB-Ia. *Haplophragmoides* spp. are generally identified as occupants of the high and middle marsh (Jennings and Nelson, 1992; Guilbault et al., 1996; Scott et al., 1996; Gehrels and van de Plassche, 1999; Patterson et al., 1999; Horton and Edwards, 2006; Kemp et al., 2009a; Hawkes et al., 2010), but it has also been found in similar highest marsh environments associated with *Trochamminita* spp. in Oregon (Hawkes et al., 2010) and British Columbia (Guilbault et al., 1996). *T. inflata* was generally absent in this zone, which is similar to the proximal Salmon River (Hawkes et al., 2010) and Alsea Bay (Nelson et al., 2008) sites, but contrasts with other Cascadia sites (Sabean, 2004; Hawkes et al., 2010).

Group SB-Ib contains foraminiferal assemblages associated with high and middle salt marshes. The group elevational range extends from 0.77 to 1.49 m MSL (1.20 ± 0.18 m). The group is dominated by *T. inflata* with *B. pseudomacrescens*, *H. wilberti* and *J. macrescens* significant contributors to the assemblage. *T. inflata* has been found in the high and middle salt marsh in studies from Cascadia (Jennings and Nelson, 1992; Nelson and Kashima, 1993; Guilbault et al., 1996; Scott et al., 1996; Nelson et al., 2008; Hawkes et al., 2010), but in contrast to results presented here is rarely the dominant species in this assemblage. It is also common along temperate coastlines on the eastern seaboard of North America (Scott and Medioli, 1978; Culver et al., 1996; Horton and Culver, 2008; Kemp et al., 2009a), Europe (Horton and Edwards, 2006) and Australasia (Horton et al., 2003; Southall et al., 2006;

Callard et al., 2011). It has previously been suggested that *J. macrescens* and/or *B. pseudomacrescens* (often combined as *T. macrescens*) form a dominant or monospecific assemblage at the limit of tidal inundation (Scott and Medioli, 1978; Scott and Medioli, 1980; Edwards et al., 2004; Hayward et al., 2004; Horton and Edwards, 2006) in contrast to their presence in the middle and high marsh at Siletz Bay.

Group SB-II represents the foraminiferal assemblages found in the tidal flat and low salt marsh environments that is always identified from MHW to below MSL with an unknown lower limit (elevational range -0.43 to 0.91 m MSL (0.32 ± 0.35 m). This zone is dominated in high abundances by *M. fusca* (> 45%). This species is found in all studies along the Pacific coast. In contrast, *M. fusca* is dominant only in the low marsh environment along the North American Atlantic coast (Wright et al., 2011) and is replaced by calcareous foraminifera on the tidal flats (Kemp et al., 2009a). This assemblage is also seen in worldwide distributions (Hayward and Hollis, 1994; Horton, 1999; Murray and Alve, 1999). Calcareous foraminifera represented by *Ammonia parkinsoniana* and *Elphidium* spp. were only present in low abundances (< 10%) in the tidal flats at Siletz Bay. This is consistent with selected published data from Cascadia (Jennings and Nelson, 1992; Guilbault et al., 1996; Shennan et al., 1996; Patterson et al., 2005; Nelson et al., 2008; Hawkes et al., 2010) but higher abundances of calcareous species have been identified in Netarts Bay (Hunger, 1966). Hawkes et al. (2010) have suggested that the absence of calcareous species may be due to the low pH of most Oregon intertidal environments.

are any found in deeper waters?

5.2 Stable carbon isotopes in bulk surface sediments

Geochemical proxies potentially have a crucial role to play in elucidating the depositional environment of a sample. TOC (Figure 8a and 8b) demonstrates a pattern of increasing values from seaward tidal flat and low marsh to highest marsh communities. This is likely due to both a decreasing input of minerogenic material with distance from open water, an increase in the total amount of biomass preservation, due to reduced flushing of the system with decreasing tidal inundation and *in-situ* organic growth (Brain et al., 2011). C:N ratios also show a relationship with elevation (Figure 8) and $\delta^{13}C$ (Figure 9), but are not suitable for reconstructions due to a tendency for upland and marsh environment values to converge (Goni and Thomas, 2000; Kemp et al., 2010; Kemp et al., 2012). This may be due to marine input of carbon from algae, POC, and DOC (Cifuentes, 1991; Lamb et al., 2006) or selective diagenesis of carbon over immobile nitrogen (Chmura et al., 1987; Ember et al., 1987). This limitation of C:N ratios has previously been observed at west coast estuarine systems including San Francisco Bay (e.g., Cloern et al., 2002). Unlike previous studies (CHV please add appropriate refs here) C:N is not able to distinguish between tidal flat and low marsh sediments; the ranges also overlap for the low marsh and tidal flat group (SB-G-III) and middle and high marsh group (SB-G-II).

If floral zones can be recognized based upon the $\delta^{13}C$ of bulk sediment, then geochemistry has potential as a sea-level indicator. Previous research has shown

so wh not just use this instead of delta carbon...this is simple and cheap

SEE: IS IT CHRIS? THE PREP IS THE SAME AS FAR AS I'M AWARE AND I THINK THE CAVEAT IN THE NEXT LINE COVERS WHY WE DON'T USE IT OVER 13C that the dominant control on the $\delta^{13}C$ values of bulk sediment is the proximal vegetation communities (Chmura and Aharon, 1995; Malamud-Roam and Ingram, 2001; Lamb et al., 2006; Lamb et al., 2007), although differential decomposition may produce sediments with lower $\delta^{13}C$ values than the local vascular plant material (Buchan et al., 2003; Vane et al., 2003; Lamb et al., 2007). The vegetation assemblage of geochemical group SB-G-I is solely C_3 vascular plants (*P. palustris*, *Gaultheria* spp., *Juncus* spp., *T. maritima, Picea* spp., *C. maculatum* and ferns). The group elevational range extends from 1.18 to 1.60 m MSL (1.30 ± 0.14 m). All samples within these zones had $\delta^{13}C$ values less than -28.5‰. This is significantly lower than has been found at other highest high marsh and freshwater zones in North America. Bulk sediment from freshwater environments in San Francisco bay had $\delta^{13}C$ values from -23.3 to -27.2‰ (Cloern et al., 2002), freshwater marshes in Louisiana had an average value of -27.8‰ (Chmura et al., 1987) and four upland samples from New Jersey ranged from -25.1 to -26.5‰. (Kemp et al., 2012) found $\delta^{13}C$ values of -22 to -27‰ in the brackish transition zone in New Jersey. The values presented here are even further removed from a result of -24.5‰ obtained from upland border sediments in Massachusetts (Middleburg et al., 1997). However, the results are consistent with the $\delta^{13}C$ values for plant material of the dominant vegetation types found in the highest high marsh and terrestrial environments at Siletz that range from -28.3 to -29.6‰ (Table 2). This result highlights the importance of collecting local bulk sediment samples when undertaking paleoenvironmental reconstructions using $\delta^{13}C$. The $\delta^{13}C$ values for this group are consistent with those for foraminiferal group SB-Ia (-29.6 ± 0.8‰ and -29.5 ±

0.6‰, respectively). TOC values (24.5 to 39.0%) are higher than found in 6 samples from New Jersey (Kemp et al., 2012) freshwater sediments (<10%) but consistent with values found at the freshwater/salt marsh boundary (2 to 35%). C:N ratios are also higher at Siletz Bay(16.9 to 28.0) than found in either of these environments in New Jersey (12 to 16; Kemp et al., 2012).

Geochemical group SB-G-II is composed of C_3 (*Agrostis* spp., *Juncus* spp. and *S. virginica)* with sparse presence of C_4 (*D. spicata*) vascular plants. The group elevational range extends from 0.16 to 1.60 m MSL (1.19 ± 0.35 m). A number of samples that were classified within foraminiferal group SB-Ib are not found in geochemical group SB-G-II. The effect of this can be seen in the difference between the bulk sediment $\delta^{13}C$ for the foraminiferal (-25.6 ± 2.0‰) and geochemical (-27.3 ± 1.4‰) groups. This is driven by the species *D. spicata*. Removing samples dominated by this species (>50%) in the foraminiferal derived groups results in a bulk $\delta^{13}C$ of -26.7 ± 1.8‰ in greater agreement with the geochemical group.

Geochemical group SB-G-III is composed of tidal flats (unvegetated or sparsely covered with *Z. nana)*, low marsh (*Scirpus* spp. and/or *C. lyngbyei*) and middle marsh (*D. spicata* and *S. virginica*). The group elevational range extends from -0.43 to 1.24 m MSL (0.48 ± 0.44 m). *C. lyngbyei* plant material has a low $\delta^{13}C$ value (-28.0‰ (Wooller et al., 2007); Table 2). The dominant effect of local vegetation on bulk sediment $\delta^{13}C$ values is again seen in this group. Compared to an average bulk sediment $\delta^{13}C$ value of -24.1 ± 1.7‰, samples not associated with *C. lyngbyei* have a lower value of -23.9 ± 1.6‰ in contrast to samples in a dominant *C. lyngbyei* vegetation zone (-26.6 ± 1.6‰). This is also reflected in greater TOC (2.8 ± 1.4 and 2.5 ± 1.8%) and C:N (11.6 ± 2.0 and 10.3 ± 2.7) values although there is significant overlap.

5.3 Application of salt marsh foraminifera and stable carbon isotopes to reconstruct coseismic land level change

The coastline of Cascadia is subject to a major seismic hazard as the Juan de Fuca plate subducts beneath North America (Clague, 1997). This is recorded in coastal stratigraphic sequences as tidal flats, grading upwards into organic tidal marsh or upland soil deposits. When the strain builds to a point where the plate boundary ruptures, the North American plate responds elastically and the coast of Cascadia subsides almost instantaneously while areas formerly locked rebound. This is archived at the coastline as an abrupt stratigraphic boundary due to the organic deposits dropping lower in the tidal frame (Nelson et al., 1996b; Atwater and Hemphill-Haley, 1997; Kelsey et al., 2002; Witter et al., 2003; Hawkes et al., 2011). The plates once again become locked, strain starts to build and the cycle recommences.

Stable carbon isotopes may provide an alternative solution to microfossil-based methods to reconstruct the magnitude of coseismic subsidence due to a great earthquake. To test the utility of this method we compared the reconstructions produced by the new geochemical plus qualitative foraminifera method with those produced using the foraminiferal zonations presented in this paper to a record of the AD 1700 earthquake (Atwater et al., 2005) from Siletz Bay .

At Salishan Spit, we sampled a vibracore taken towards the rear of the salt marsh. Five foraminiferal and geochemical samples (Figure 10) were taken across the AD 1700 contact in core SSV2 in Siletz Bay (Figure 1C). In core SSV2 at 60 cm depth there is an abrupt (< 1mm) contact between underlying organic sandy silt and an overlying upward fining silty sand unit interpreted as a tsunami deposit. A silty clay unit in turn overlies this. The three foraminiferal samples below the contact have high abundances of agglutinated foraminifera, dominated by *B. pseudomacrescens* (60 to 82%) with low to absent *M. fusca* (0 to 3%) and *T. irregularis* (0 to 3%). These indicate that the sample formed in the middle/high marsh environment (SB-Ib). $\delta^{13}C$ values range from -25.7 to -26.2‰ indicating that the marsh formed in geochemical zone SB-G-II. This is further supported by TOC (11.0 to 11.8%) and C:N ratios (13.4 to 13.8). The first sample in the silty clay unit is predominantly *M. fusca* (59%). This indicates that the sample formed in the low marsh/tidal flat group SB-II. The $\delta^{13}C$ increased to -24.6‰ and TOC reduced to 7.7% indicative of formation in geochemical zone SB-G-III. The C:N ratio (12.6) is inconclusive for this sample. The magnitude of subsidence for both methods can be calculated by subtracting the difference between the center points of the elevations of groups. For foraminifera:

Coseismic Subsidence = SB-Ib – SB-II

= 1.20m MSL – 0.32m MSL

= 0.88m

The error is calculated by taking the square root of the sum of half the ranges of groups SB-Ib and SB-II:

Error = $\sum (0.18m^2 + 0.35m^2)$

= ± 0.39m

And for stable carbon isotopes:

Coseismic Subsidence = SB-G-II – SB-G-III

= 1.19m MSL – 0.48m MSL

= 0.71m

Error = $\sum (0.35m^2 + 0.44m^2)$

= ± 0.56m

Both methods produce estimates that overlap, providing some measure of confidence in the ability of the carbon isotope technique. Both methods produce results that equivocally confirm subsidence with minimum estimates greater than 0m (0.49m versus 0.15m) and are above the threshold values of 0.5m (Nelson et al., 1996a) used to definitively ascribe the subsidence to a megathrust earthquake.

Indeed, the correlation of the AD 1700 soil and a high tsunami from over 900 km of the Cascadia coastline (Atwater et al., 1995; Nelson et al., 1995; Clague et al., 2000; Nelson et al., 2006) allows us to ascribe the subsidence to a megathrust earthquake. The estimates from both methods are consistent with the previous value obtained for the Siletz site by Darienzo et al. (1994) of 0.5 to 1.0 m using a qualitative interpretation based on plant macrofossils and lithology.

6. Conclusions

We documented the distribution of salt-marsh foraminifera and $\delta^{13}C$, TOC and C:N from four transect, at three salt marshes with differing salinity regimes in Siletz Bay, Oregon. We used PAM to identify elevation-dependent ecological zones, which are similar to those observed at other sites in Cascadia as well as globally. The highest marsh occupies a narrow elevational range and is dominated by T. irregularis. High and middle marsh environments are dominated by T. inflata with B. pseudomacrescens, H. wilberti and J. macrescens. Low marsh environments form near monospecific assemblages with M. fusca. Calcareous taxa are limited in the tidal flat (< 10%). PAM analysis of the $\delta^{13}C$, TOC and C:N also revealed three elevation dependent zones, which broadly correspond to those identified by foraminifera. The highest marsh is defined by low $\delta^{13}C$ (-29.6 ± 0.8‰), high TOC (30 ± 4.6%) and high C:N (20.4 ± 3.7). The high and middle marsh are identified by $\delta^{13}C$ of -27.3 ± 1.4‰, TOC of 12.4 ± 4.0% and C:N of 13.6 ± 1.4. The low marsh and tidal flat had the highest $\delta^{13}C$ (-24.1 ± 1.7‰), lowest TOC (2.5 ± 1.8%) and lowest C:N (10.4 ± 2.7) values. Lower $\delta^{13}C$ values than are found in similar environments in

North America highlight the importance of collecting a local dataset of bulk sediments for geochemical analysis.

The sub-division of the dataset into elevation dependent ecological zones allows the use of both foraminifera and $\delta^{13}C$ (supported by TOC and C:N) as indicators of former sea level that can infer the amount of coseismic subsidence associated with megathrust earthquakes in Cascadia. We tested this by applying both methods to a record of the AD 1700 earthquake taken from Salishan spit. Foraminifera and geochemical analyses produced similar estimates of subsidence (0.88 ± 0.39m and 0.71 ± 0.56m, respectively), providing a measure of confidence in the new semi-quantitative $\delta^{13}C$ technique. This approach provides a new method to obtain estimates of coseismic subsidence quickly before quantitative foraminiferal analysis and/or when microfossil abundances are not appropriate for quantitative analysis (e.g., transfer functions).

7. Acknowledgements

This research was supported by an NSF grant (EAR-0842728) to BPH. This paper is a contribution to IGCP Project 588. The Siletz Bay National Wildlife Refuge and the Salishan Leaseholders, Inc community are thanked for allowing access to the sites. Rich Briggs and Harvey Kelsey are thanked for assistance in the field. David Hill provided the tidal predictions used in this paper.

Published in Paleo3, (2013) 377,13-27

Figure Captions

Figure 1. Map of (A) the Cascadia subduction zone (USA) showing the location of Siletz Bay. Black circles mark the sites identified in Figure 5 (B) the location of three sites within Siletz Bay that were sampled for foraminifera and geochemistry (C) Salishan Spit, (D) Siletz East, and (E) Millport Slough. A core (SSV2) was collected from Salishan Spit (C)

Figure 2. Elevation profile of transects at A) Salishan Spit transect 1, B) Salishan Spit transect 2, C) Siletz East and D) Millport Slough. Vegetation zones correspond to Table 1. Distribution of dominant foraminifera along each transect in % with only dominant species being shown. SW = *Picea* spp. swamp; HHM = highest marsh; HM = high marsh; MM = middle marsh; LM = low marsh; TF = tidal flat.

Figure 3. Relative abundance of dead foraminifera at Salishan Spit transect 1 (SS). PAM cluster analysis sub-divides the data into two groups, SS-I (black bars) and SS-II (white bars). Silhouette plot for PAM clustering of foraminiferal samples partitioned into two groups. The silhouette plot shows widths between -1 and 1, where values close to -1 indicate that a sample was incorrectly classified and values close to 1 indicate that a sample was assigned to an appropriate group.

Figure 4. Elevation profile of transects at A) Salishan Spit transect 1, B) Salishan Spit transect 2, C) Siletz East, and D) Millport Slough. Vegetation zones correspond to Table 1. Distribution of $\delta^{13}C$, total organic carbon (TOC) and C:N ratios along each transect are shown. SW = *Picea* spp. swamp; HHM = highest marsh; HM = high marsh; MM = middle marsh; LM = low marsh; TF = tidal flat.

Figure 5. Relative abundance of dead foraminifera when combined into a single Siletz Bay dataset. PAM cluster analysis sub-divides the data into three groups, SB-Ia (grey bars), SB-Ib (black bars) and SB-II (white bars). Silhouette plot for PAM clustering of foraminiferal samples partitioned into three groups. The silhouette plot shows widths between -1 and 1, where values close to -1 indicate that a sample was incorrectly classified and values close to 1 indicate that a sample was assigned to an appropriate group.

Figure 6. Stable carbon isotope values when combined into a single Siletz Bay dataset. PAM cluster analysis sub-divides the data into three groups, SB-G-I (grey bars), SB-G-II (black bars) and SB-G-III (white bars). Silhouette plot for PAM grouping of stable carbon isotope samples partitioned into three groups. The silhouette plot shows widths between -1 and 1, where values close to -1 indicate that a sample was incorrectly classified and values close to 1 indicate that a sample was assigned to an appropriate group.

Figure 7. Distribution and elevational ranges of dominant foraminifera from Siletz Bay compared to other studies from Cascadia (Guilbault et al., 1996; Sabean, 2004; Patterson et al., 2005; Nelson et al., 2008; Hawkes et al., 2010). Aspp = *Ammobaculites* spp.; Bp = *Balticammina pseudomacrescens*; Hm = *Haplophragmoides manilaensis*; Hw = *Haplophragmoides wilberti*; Hspp = *Haplophragmoides* spp.; Jm = *Jadammina macrescens*; Mf = *Miliammina fusca*; Ti = *Trochammina inflata*; Tm = *Trochammina macrescens*; Tr = *Trochamminita irregularis*; Ts = *Trochamminita salsa*. Solid line indicates minimal elevational overlap between groups. A dashed line indicates overlap between groups. Elevational ranges are shown in detail for the data presented here. Ranges are presented as box and whisker plots, where the box is the mean ± one standard deviation and the whiskers represent the minimum and maximum elevation in each group.

Figure 8. (A). The associated mean ± one standard deviation in $\delta^{13}C$, C:N ratios, total organic content (TOC), and elevations for the modern samples based on the foraminiferal groups. (B) The associated mean ± one standard deviations in $\delta^{13}C$, C:N ratios, total organic content (TOC), and elevations for the modern samples based on the geochemistry groups. Ranges are presented as box and whisker plots, where the box is the mean ± one standard deviation and the whiskers represent the maximum and minimum in each group.

Figure 9. $\delta^{13}C$ and C:N values in bulk organic sediment from sampling stations in Siletz Bay, Oregon. Samples are sub-divided by stable carbon isotope groups identified by PAM.

Figure 10. Stratigraphy (including lithology and type of contact), foraminiferal assemblages, $\delta^{13}C$ and results of semi-quantitative foraminifera and geochemistry analysis reconstruction of the paleomarsh elevations in the sediment sequence bisecting the AD 1700 earthquake in core SSV2 taken at Salishan Spit in Siletz Bay. The calculated coseismic subsidence with the error in meters marked on both reconstructions.

Table 1. Vascular plant zonations and foraminiferal associations at the three studied sites in Siletz Bay. Bp = *Balticammina pseudomacrescens*; Hm = *Haplophragmoides manilaensis*; Hw = *Haplophragmoides wilberti*; Jm = *Jadammina macrescens*; Mf = *Miliammina fusca*; Ti = *Trochammina inflata*; Tr = *Trochamminita irregularis*

Site	Marsh Type	Vegetation	Foraminifera
Salishan Spit	Highest Marsh	*Gaultheria* spp., *Potentilla palustris*, *Juncus* spp. *Picea* spp., Ferns	Tr
	High Marsh	*Agrostis* spp., *Salicornia virginica*, *Juncus* spp., *Distichlis spicata*, *Potentilla palustris*	Ti, Hw, Hm
	Middle Marsh	*Distichlis spicata*, *Salicornia virginica*	Ti, Jm, Hw, Mf
	Low Marsh	*Scirpus* spp.	Mf
	Tidal Flat	*Zostera nana*	Mf
Siletz East	High Marsh	*Agrostis* spp., *Juncus* spp., *Distichlis spicata*	Ti, Jm, Bp, Hw
	Low Marsh	*Carex lyngbyei*	Mf
	Tidal Flat	Unvegetated	Mf
Millport Slough	Swamp	*Picea* spp.	Tr, Hw, Jm, Bp
	High Marsh	*Potentilla palustris*, *Triglochin maritima*, *Juncus* spp.	Tr, Hw, Hm, Bp, Mp
	Low Marsh	*Carex lyngbyei*	Mf

Table 2. Published δ13C values for salt marsh species found in the marshes of Siletz Bay and discussed in this study

Vegetation	Typical $\delta^{13}C$ Value (‰)	Reference
Zostera nana/japonica	-12.4	Thayer et al. 1978
Scirpus maritimus	-25.5	Byrne et al. 2001
Carex lyngbyei	-28.0	Wooler et al. 2007
Distichlis spicata	-12.7	Byrne et al. 2001
Salicornia virginica	-27.2	Byrne et al. 2001
Juncus balticus	-28.4	Byrne et al. 2001
Agrostis capilaris/gigantea	-25.99	Wedin et al. 1995
Triglochin maritima	-28.3	Cloern et al. 2002
Potentilla palustris	-29.6	Brooks et al. 1997
Gaultheria shallon/salal	-29.4	Brooks et al. 1997

Table 3. Elevational ranges for six environmental groups defined at Siletz Bay on the basis of foraminifera (SB-Ia, SB-Ib and SB-II) and geochemistry (SB-G-I, SB-G-II and SB-G-III). MSL = mean sea level.

Group	**Foraminifera**	**$\delta^{13}C$ (‰)**	**Elevation (m MSL)**
SB-Ia	Agglutinated foraminifera of which >25% *T. irregularis*	-29.5 ± 0.6	1.36 ± 0.15
SB-Ib	Agglutinated foraminifera of which <45% *M. fusca*	-25.6 ± 2.0	1.20 ± 0.18
SB-II	Agglutinated foraminifera of which >45% *M. fusca*	-24.4 ± 1.8	0.32 ± 0.35
SB-G-I	Agglutinated foraminifera present	*-29.6 ± 0.8*	1.30 ± 0.14
SB-G-II	Agglutinated foraminifera present	*-27.3 ± 1.4*	1.19 ± 0.35
SB-G-III	Not required	*-24.1 ± 1.7*	0.48 ± 0.44

8. References

Atwater, B.F., 1987. Evidence for Great Holocene Earthquakes Along the Outer Coast of Washington-State. Science 236, 942-944.

Atwater, B.F., Hemphill-Haley, E., 1997. Recurrence intervals for great earthquakes of the past 3500 years at northeastern Willapa Bay, Washington. U.S. Geological Survey Professional Paper 1576, 108 p.

Atwater, B.F., Musumi-Rokkaku, S., Satake, K., Tsuji, Y., Ueda, K., Yamaguchi, D.K., 2005. The orphan tsunami of 1700 - Japanese clues to a parent earthquakes in North America. U.S. Geological Survey Professional Paper 1707, 133 p.

Atwater, B.F., Nelson, A.R., Clague, J.J., Carver, G.A., Bobrowsky, P.T., Bourgeois, J., Darienzo, M.E., Grant, W.C., Hemphill-Haley, E., Kelsey, H.M., Jacoby, C.G., Nishenko, S.P., Palmer, S., Peterson, C.D., Reinhart, M.A., Yamaguchi, D.K., 1995. Summary of coastal geologic evidence for past great earthquakes at the Cascadia subduction zone. Earthquake Spectra 11, 1-18.

Bottom, D., Kreag, B., Ratti, F., Roye, C., Starr, R., 1979. Habitat classification and inventory methods for the management of Oregon estuaries, in: Wildlife, O.D.o.F.a. (Ed.), Portland, p. 109 pp.

Brain, M.J., Long, A.J., Petley, D.N., Horton, B.P., Allison, R.J., 2011. Compression behaviour of minerogenic low energy intertidal sediments. Sedimentary Geology 233, 28-41.

Brophy, L.S., Cornu, C.E., Adamus, P.R., Christy, J.A., Gray, A., Huang, L., MacClellan, M.A., Doumbia, J.A., Tully, R.L., 2011. New tools for tidal wetland restoration: development of a reference conditions database and a temperature sensor method for detecting tidal inundation in least-disturbed tidal wetlands of Oregon, USA. Prepared for the Cooperative Institute for Coastal and Estuarine Environmental Technology (CICEET), p. 150 pp.

Buchan, A., Newell, S.Y., Butler, M., Biers, E.J., Hollibaugh, J.T., Moran, M.A., 2003. Dynamics of bacterial and fungal communities on decaying salt marsh grass. Applied and Environmental Microbiology 69, 6676-6687.

Callard, S.L., Gehrels, W.R., Morrison, B.V., Grenfell, H.R., 2011. Suitability of salt-marsh foraminifera as proxy indicators of sea level in Tasmania. Marine Micropaleontology 79, 121-131.

Charland, J., W., Priest, G.R., 1995. Inventory of critical and essential facilities vulnerable to earthquake or tsunami hazards on the Oregon coast, in: Industries, O.D.o.G.a.M. (Ed.), p. 52 pp.

Published in Paleo3, (2013) 377,13-27

Chmura, G.L., Aharon, P., 1995. Stable Carbon-Isotope Signatures of Sedimentary Carbon in Coastal Wetlands as Indicators of Salinity Regime. Journal of Coastal Research 11, 124-135.

Chmura, G.L., Aharon, P., Socki, R.A., Abernethy, R., 1987. An Inventory of C-13 Abundances in Coastal Wetlands of Louisiana, USA - Vegetation and Sediments. Oecologia 74, 264-271.

Cifuentes, L.A., 1991. Spatial and Temporal Variations in Terrestrially-Derived Organic-Matter from Sediments of the Delaware Estuary. Estuaries 14, 414-429.

Clague, J.J., 1997. Evidence for large earthquakes at the Cascadia subduction zone. Rev Geophys 35, 439-460.

Clague, J.J., Bobrowsky, P.T., Hutchinson, I., 2000. A review of geological records of large tsunamis at Vancouver Island, British Columbia, and implications for hazard. Quaternary Science Reviews 19, 849-863.

Cloern, J.E., Canuel, E.A., Harris, D., 2002. Stable carbon and nitrogen isotope composition of aquatic and terrestrial plants of the San Francisco Bay estuarine system. Limnol Oceanogr 47, 713-729.

Culver, S.J., Horton, B.P., 2005. Infaunal marsh foraminifera from the outer banks, North Carolina, USA. J Foramin Res 35, 148-170.

Culver, S.J., Woo, H.J., Oertel, G.F., Buzas, M.A., 1996. Foraminifera of coastal depositional environments, Virginia, U.S.A.: distribution and taphonomy. Palaios 11, 459-486.

Darienzo, M.E., Peterson, C.D., 1995. Magnitude and frequency of subduction-zone earthquakes along the northern Oregon coast in the past 3,000 years. Oregon Geology 57, 3-12.

Edwards, R.J., 2006. Mid- to late-Holocene relative sea-level change in southwest Britain and the influence of sediment compaction. Holocene 16, 575-587.

Edwards, R.J., Wright, A., Van de Plassche, O., 2004. Surface distributions of salt-marsh foraminifera from Connecticut, USA: modem analogues for high-resolution sea level studies. Marine Micropaleontology 51, 1-21.

Eilers, H.P., 1975. Plants, plant communities, net production and tide levels: the ecological biogeography of the Nehalem salt marshes, Tillamook County, Oregon. Oregon State University, Corvallis, p. 368.

Ember, L.M., Williams, D.F., Morris, J.T., 1987. Processes that influence carbon isotope variations in salt marsh sediments. Marine Ecology Progress Series 36, 33-42.

Frankel, A.D., Petersen, M.D., Mueller, C.S., Haller, K.M., Wheeler, R.L., Leyendecker, E.V., Wesson, R.L., Harmsen, S.C., Cramer, C.H., Perkins, D.M., Rukstales, K.S., 2002. Documentation for the 2002 update of the national seismic hazard maps, in: Survey, U.S.G. (Ed.), p. 33 pp.

Gallagher, J.L., Kibby, H.V., 1980. Marsh Plants as Vectors in Trace-Metal Transport in Oregon Tidal Marshes. American Journal of Botany 67, 1069-1074.

Gehrels, W.R., 1994. Determining Relative Sea-Level Change from Salt-Marsh Foraminifera and Plant Zones on the Coast of Maine, USA. Journal of Coastal Research 10, 990-1009.

Gehrels, W.R., Belknap, D.F., Black, S., Newnham, R.M., 2002. Rapid sea-level rise in the Gulf of Maine, USA, since AD 1800. Holocene 12, 383-389.

Gehrels, W.R., Milne, G.A., Kirby, J.R., Patterson, R.T., Belknap, D.F., 2004. Late Holocene sea-level changes and isostatic crustal movements in Atlantic Canada. Quatern Int 120, 79-89.

Gehrels, W.R., Roe, H.M., Charman, D.J., 2001. Foraminifera, testate amoebae and diatoms as sea-level indicators in UK saltmarshes: a quantitative multiproxy approach. Journal of Quaternary Science 16, 201-220.

Gehrels, W.R., van de Plassche, O., 1999. The use of Jadammina macrescens (Brady) and Balticammina pseudomacrescens Bronnimann, Lutze and Whittaker (Protozoa : Foraminiferida) as sea-level indicators. Palaeogeogr Palaeocl 149, 89-101.

Goni, M.A., Thomas, K.A., 2000. Sources and transformations of organic matter in surface soils and sediments from a tidal estuary (north inlet, South Carolina, USA). Estuaries 23, 548-564.

Gonzalez, J.L., Tornqvist, T.E., 2009. A new Late Holocene sea-level record from the Mississippi Delta: evidence for a climate/sea level connection? Quaternary Science Reviews 28, 1737-1749.

Guilbault, J.-P., Clague, J.J., Lapointe, M., 1996. Foraminiferal evidene for the amount of coseismic subsidence during a late Holocene earhquake on Vancouver Island, west coast of Canada. Quaternary Science Reviews 15, 913-937.

Guilbault, J.P., Clague, J.J., Lapointe, M., 1995. Amount of Subsidence during a Late Holocene Earthquake - Evidence from Fossil Tidal Marsh Foraminifera at Vancouver-Island, West-Coast of Canada. Palaeogeogr Palaeocl 118, 49-71.

Hawkes, A.D., 2008. The application of foraminifera to characterize tsunami sediment and quantify coseismic subsidence along the Sumatra and Cascadia subduction zones, Department of Earth and Environmental Science. University of Pennsylvania, Philadelphia, p. 215 pp.

Hawkes, A.D., Horton, B.P., Nelson, A.R., Hill, D.F., 2010. The application of intertidal foraminifera to reconstruct coastal subsidence during the giant Cascadia earthquake of AD 1700 in Oregon, USA. Quatern Int 221, 116-140.

Hawkes, A.D., Horton, B.P., Nelson, A.R., Vane, C.H., Sawai, Y., 2011. Coastal subsidence in Oregon, USA, during the giant Cascadia earthquake of AD 1700. Quaternary Science Reviews 30, 364-376.

Hayward, B.W., Hollis, C.J., 1994. Brackish Foraminifera in New-Zealand - a Taxonomic and Ecologic Review. Micropaleontology 40, 185-222.

Hayward, B.W., Scott, G.H., Grenfell, H.R., Carter, R., Lipps, J.H., 2004. Techniques for estimation of tidal elevation and confinement (salinity) histories of sheltered harbours and estuaries using benthic foraminifera: examples from New Zealand. The Holocene 14, 218-232.

Hemphill-Haley, E., 1995. Diatom evidence for earthquake-induced subsidence and tsunami 300 years ago in southern coastal Washington. Geol Soc Am Bull 107, 367-378.

Horton, B.P., 1999. The distribution of contemporary intertidal foraminifera at Cowpen Marsh, Tees Estuary, UK: implications for studies of Holocene sea-level changes. Palaeogeogr Palaeocl 149, 127-149.

Horton, B.P., Culver, S.J., 2008. Modern intertidal foraminifera of the Outer Banks, North Carolina, USA, and their applicability for sea-level studies. Journal of Coastal Research 24, 1110-1125.

Horton, B.P., Edwards, R.J., 2005. The application of local and regional transfer functions to the reconstruction of Holocene sea levels, north Norfolk, England. Holocene 15, 216-228.

Horton, B.P., Edwards, R.J., 2006. Quantifying Holocene sea-level change using intertidal foraminifera: lessons for the British Isles. Cushman Foundation for Foraminiferal Research Special Publication, 40, 97p.

Horton, B.P., Larcombe, P., Woodroffe, S.A., Whittaker, J.E., Wright, M.R., Wynn, C., 2003. Contemporary foraminiferal distributions of a mangrove environment, Great Barrier Reef coastline, Australia: implications for sea-level reconstructions. Marine Geology 198, 225-243.

Horton, B.P., Peltier, W.R., Culver, S.J., Drummond, R., Engelhart, S.E., Kemp, A.C., Mallinson, D., Thieler, E.R., Riggs, S.R., Ames, D.V., Thomson, K.H., 2009. Holocene sea-level changes along the North Carolina Coastline and their implications for glacial isostatic adjustment models. Quaternary Science Reviews 28, 1725-1736.

Hughes, J.F., Mathewes, R.W., Clague, J.J., 2002. Use of pollen and vascular plants to estimate coseismic subsidence at a tidal marsh near Tofino, British Columbia. Palaeogeogr Palaeocl 185, 145-161.

Hunger, A.A., 1966. Distribution of foraminifera, Netarts Bay, Oregon. Oregon State University, Corvallis.

Jefferson, C.A., 1975. Plant communities and succession in Oregon coastal salt marshes. Oregon State University, Corvallis, p. 192.

Jennings, A.E., Nelson, A.R., 1992. Foraminiferal Assemblage Zones in Oregon Tidal Marshes - Relation to Marsh Floral Zones and Sea-Level. J Foramin Res 22, 13-29.

Jennings, A.E., Nelson, A.R., Scott, D.B., Aravena, J.C., 1995. Marsh Foraminiferal Assemblages in the Valdivia Estuary, South-Central Chile, Relative to Vascular Plants and Sea-Level. Journal of Coastal Research 11, 107-123.

Kaufman, L., Rousseeuw, P.J., 1990. Finding groups in data: an introduction to cluster analysis. Wiley-Interscience.

Kelsey, H.M., Witter, R.C., Hemphill-Haley, E., 2002. Plate-boundary earthquakes and tsunamis of the past 5500 yr, Sixes River estuary, southern Oregon. Geol Soc Am Bull 114, 298-314.

Kemp, A.C., Horton, B.P., Culver, S.J., 2009a. Distribution of modern salt-marsh foraminifera in the Albemarle-Pamlico estuarine system of North Carolina, USA: Implications for sea-level research. Marine Micropaleontology 72, 222-238.

Kemp, A.C., Horton, B.P., Culver, S.J., Corbett, D.R., van de Plassche, O., Gehrels, W.R., Douglas, B.C., Parnell, A.C., 2009b. Timing and magnitude of recent accelerated sea-level rise (North Carolina, United States). Geology 37, 1035-1038.

Kemp, A.C., Horton, B.P., Donnelly, J.P., Mann, M.E., Vermeer, M., Rahmstorf, S., 2011. Climate related sea-level variations over the past two millennia. P Natl Acad Sci USA 108, 11017-11022.

Kemp, A.C., Horton, B.P., Vann, D.R., Engelhart, S.E., Grand-Pre, C., Vane, C.H., Nikitina, D., Anisfeld, S.C., In Press. Quantitative vertical zonation of salt-marsh foraminifera for reconstructing former sea level; an example from New Jersey, USA. Quaternary Science Reviews.

Kemp, A.C., Vane, C., Horton, B.P., Culver, S.J., 2010. Stable carbon isotopes as potential sea-level indicators in salt marshes, North Carolina, USA. The Holocene 20, 623-636.

Kemp, A.C., Vane, C.H., Horton, B.P., Engelhart, S.E., Nikitina, D., 2012. Application of stable carbon isotopes for reconstructing salt-marsh floral zones and relative sea level, New Jersey, USA. Journal of Quaternary Science 27, 404-414.

Lamb, A.L., Vane, C.H., Wilson, G.P., Rees, J.G., Moss-Hayes, V.L., 2007. Assessing δ13C and C/N ratios from organic material archived in cores as Holocene sea level and palaeoenvironmental indicators in the Humber Estuary, UK. Marine Geology 244, 109-128.

Lamb, A.L., Wilson, G.P., Leng, M.J., 2006. A review of coastal palaeoclimate and relative sea-level reconstructions using delta C-13 and C/N ratios in organic material. Earth-Science Reviews 75, 29-57.

Leorri, E., Martin, R., McLaughlin, P., 2006. Holocene environmental and parasequence development of the St. Jones Estuary, Delaware (USA): Foraminiferal proxies of natural climatic and anthropogenic change. Palaeogeography, Palaeoclimatology, Palaeoecology 241, 590-607.

Lloyd, J.M., Evans, J.R., 2002. Contemporary and fossil foraminifera from isolation basins in northwest Scotland. Journal of Quaternary Science 17, 431-443.

Mackie, E.A.V., Lloyd, J.M., Leng, M., Bentley, M.J., Arrowsmith, C., 2007. Assessment of delta C-13 and C/N ratios in bulk organic matter as palaeosalinity indicators in Holocene and Lateglacial isolation basin sediments, northwest Scotland. Journal of Quaternary Science 22, 579-591.

Maechler, M., Rousseeuw, P., Struyf, A., Hubert, M., 2005. Cluster Analysis Basics and Extensions.

Malamud-Roam, F., Ingram, B.L., 2001. Carbon isotopic compositions of plants and sediments of tide marshes in the San Francisco Estuary. Journal of Coastal Research 17, 17-29.

Middleburg, J.J., Nieuwenhuize, J., Lubberts, R.K., van de Plassche, O., 1997. Organic carbon isotope systematics of coastal marshes. Estuar Coast Shelf S 45, 681-687.

Murray, J.W., 1982. Benthic foraminifera: the variability of living, dead or total assemblages in the interpretation of palaeoecology. Journal of Micropalaeontology 1, 137-140.

Murray, J.W., Alve, E., 1999. Natural dissolution of modern shallow water benthic foraminifera: taphonomic effects on the palaeoecological record. Palaeogeogr Palaeocl 146, 195-209.

Nelson, A.R., Atwater, B.F., Bobrowsky, P.T., Bradley, L.A., Clague, J.J., Carver, G.A., Darienzo, M.E., Grant, W.C., Krueger, H.W., Sparks, R., Stafford, T.W., Stuiver, M.,

1995. Radiocarbon Evidence for Extensive Plate-Boundary Rupture About 300 Years Ago at the Cascadia Subduction Zone. Nature 378, 371-374.

Nelson, A.R., Jennings, A.E., Kashima, K., 1996a. An earthquake history derived from stratigraphic and microfossil evidence of relative sea-level change at Coos Bay, southern coastal Oregon. Geol Soc Am Bull 108.

Nelson, A.R., Kashima, K., 1993. Diatom Zonation in Southern Oregon Tidal Marshes Relative to Vascular Plants, Foraminifera, and Sea-Level. Journal of Coastal Research 9, 673-697.

Nelson, A.R., Kelsey, H.M., Witter, R.C., 2006. Great earthquakes of variable magnitude at the Cascadia subduction zone. Quaternary Research 65, 354-365.

Nelson, A.R., Sawai, Y., Jennings, A.E., Bradley, L.A., Gerson, L., Sherrod, B.L., Sabean, J., Horton, B.P., 2008. Great-earthquake paleogeodesy and tsunamis of the past 2000 years at Alsea Bay, central Oregon coast, USA. Quaternary Science Reviews 27, 747-768.

Nelson, A.R., Shennan, I., Long, A.J., 1996b. Identifying coseismic subsidence in tidal-wetland stratigraphic sequences at the Cascadia subduction zone of western North America. J Geophys Res-Sol Ea 101, 6115-6135.

Oglesby, L.C., 1968. Responses of an estuarine population of the polychaete nereis limnicola to osmotic stress. The Biological Bulletin 134, 118-138.

Patterson, R.T., Dalby, A.P., Roe, H.M., Guilbault, J.-P., Hutchinson, I., Clague, J.J., 2005. Relative utility of foraminifera, diatoms and macrophytes as high resolution indicators of paleo-sea level in coastal British Columbia, Canada. Quaternary Science Reviews 24, 2002-2014.

Patterson, R.T., Guilbault, J.P., Clague, J.J., 1999. Taphonomy of tidal marsh foraminifera: implications of surface sample thickness for high-resolution sea-level studies. Palaeogeogr Palaeocl 149, 199-211.

Petersen, M.D., Cramer, C.H., Frankel, A.D., 2002. Simulations of seismic hazard for the Pacific Northwest of the United States from earthquakes associated with the Cascadia subduction zone. Pure and Applied Geophysics 159, 2147-2168.

Peterson, C., Scheidegger, K., Komar, P., Niem, W., 1984. Sediment composition and hydrography in six high-gradient estuaries of the northwestern United States. Journal of Sedimentary Research 54, 86-97.

Peterson, C.D., Doyle, D.L., Barnett, E.T., 2000. Coastal flooding and beach retreat from coseismic subsidence in the central Cascadia margin, USA. Environmental & Engineering Geoscience 6, 255-269.

Priest, G.R., Goldfinger, C., Wang, K.L., Witter, R.C., Zhang, Y.L., Baptista, A.M., 2010. Confidence levels for tsunami-inundation limits in northern Oregon inferred from a 10,000-year history of great earthquakes at the Cascadia subduction zone. Natural Hazards 54, 27-73.

Sabean, J.A.R., 2004. Applications of foraminifera to detecting land level change associated with great earthquakes along the west coast of North America, Department of Earth Sciences. Simon Fraser University, Burnaby.

Scott, D., Medioli, F., 1980. Quantitative studies of marsh foraminiferal distributions in Nova Scotia: implications for sea level studies. Cushman Foundation for Foraminiferal Research.

Scott, D.B., Collins, E.S., Duggan, J., Asioli, A., Saito, T., Hasegawa, S., 1996. Pacific rim marsh foraminiferal distributions: Implications for sea-level studies. Journal of Coastal Research 12, 850-861.

Scott, D.B., Hermelin, J.O.R., 1993. A Device for Precision Splitting of Micropaleontological Samples in Liquid Suspension. J Paleontol 67, 151-154.

Scott, D.S., Medioli, F.S., 1978. Vertical Zonations of Marsh Foraminifera as Accurate Indicators of Former Sea-Levels. Nature 272, 528-531.

Seliskar, D.M., Gallagher, J.L., 1983. The ecology of tidal marshes of the Pacific Northwest coast: a community profile, in: U.S. Fish and Wildlife Service, D.o.B.S. (Ed.), Washington D.C., p. 65.

Shennan, I., Long, A.J., Rutherford, M.M., Green, F.M., Innes, J.B., Lloyd, J.M., Zong, Y., Walker, K.J., 1996. Tidal marsh stratigraphy, sea-level change and large earthquakes .1. A 5000 year record in Washington, USA. Quaternary Science Reviews 15, 1023-1059.

Shennan, I., Long, A.J., Rutherford, M.M., Innes, J.B., Green, F.M., Walker, K.J., 1998. Tidal marsh stratigraphy, sea-level change and large earthquakes - II: Submergence events during the last 3500 years at Netarts Bay, Oregon, USA. Quaternary Science Reviews 17, 365-393.

Sherrod, B.L., 1999. Gradient analysis of diatom assemblages in a Puget Sound salt marsh: can such assemblages be used for quantitative paleoecological reconstructions? Palaeogeogr Palaeocl 149, 213-226.

Southall, K.E., Gehrels, W.R., Hayward, B.C., 2006. Foraminifera in a New Zealand salt marsh and their suitability as sea-level indicators. Marine Micropaleontology 60, 167-179.

Tornqvist, T.E., Gonzalez, J.L., Newsom, L.A., van der Borg, K., de Jong, A.F.M., Kurnik, C.W., 2004. Deciphering Holocene sea-level history on the US Gulf Coast: A high-resolution record from the Mississippi Delta. Geol Soc Am Bull 116, 1026-1039.

Vane, C.H., Drage, T.C., Snape, C.E., 2003. Biodegredation of Oak (Quercus alba) wood during growth of the Shiitake mushroom (Lentinula edodes): A molecular approach. Journal of Agricultural and Food Chemistry 51, 947-956.

Wang, Y., Clark, J.L., 1999. Earthquake damage in Oregon, preliminary estimates of future earthquake losses, in: Industries, O.D.o.G.a.M. (Ed.), p. 59 pp.

Wilson, G.P., Lamb, A.L., Leng, M.J., Gonzalez, S., Huddart, D., 2005. Variability of organic delta C-13 and C/N in the Mersey Estuary, UK and its implications for sea-level reconstruction studies. Estuar Coast Shelf S 64, 685-698.

Witter, R.C., Kelsey, H.M., Hemphill-Haley, E., 2003. Great Cascadia earthquakes and tsunamis of the past 6700 years, Coquille River estuary, southern coastal Oregon. Geol Soc Am Bull 115, 1289-1306.

Wooller, M.J., Zazula, G.D., Edwards, M., Froese, D.G., Boone, R.D., Parker, C., Bennett, B., 2007. Stable carbon isotope compositions of Eastern Beringian grasses and sedges: Investigating their potential as paleoenvironmental indicators. Arctic Antarctic and Alpine Research 39, 318-331.

Wright, A.J., Edwards, R.J., van de Plassche, O., 2011. Reassessing transfer-function performance in sea-level reconstructions based on benthic salt-marsh foraminifera from the Atlantic coast of NE North America. Marine Micropaleontology 81, 43-62.

Published in Paleo3, (2013) 377,13-27

Figure 1

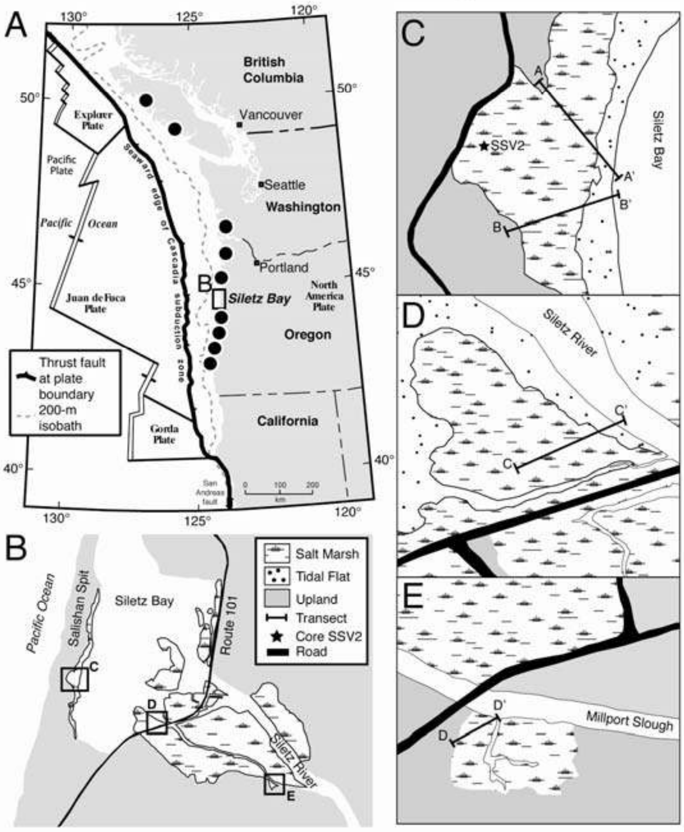

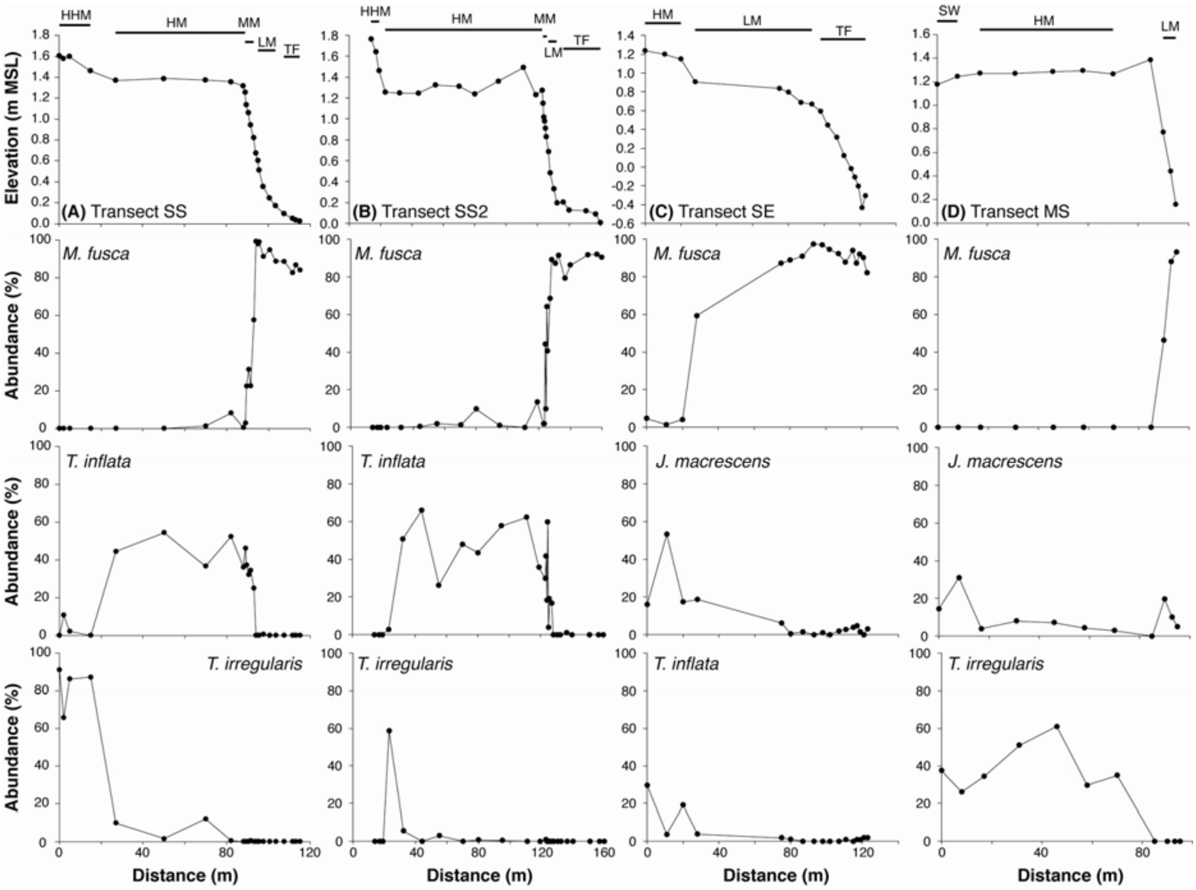

HHM
HM
MM
LM
TF
SW
Elevation (m MSL)
(A) Transect SS
(B) Transect SS2
(C) Transect SE
(D) Transect MS
Abundance (%)
M. fusca
T. inflata
J. macrescens
T. irregularis
Distance (m)

Figure 2

Published in Paleo3, (2013) 377,13-27

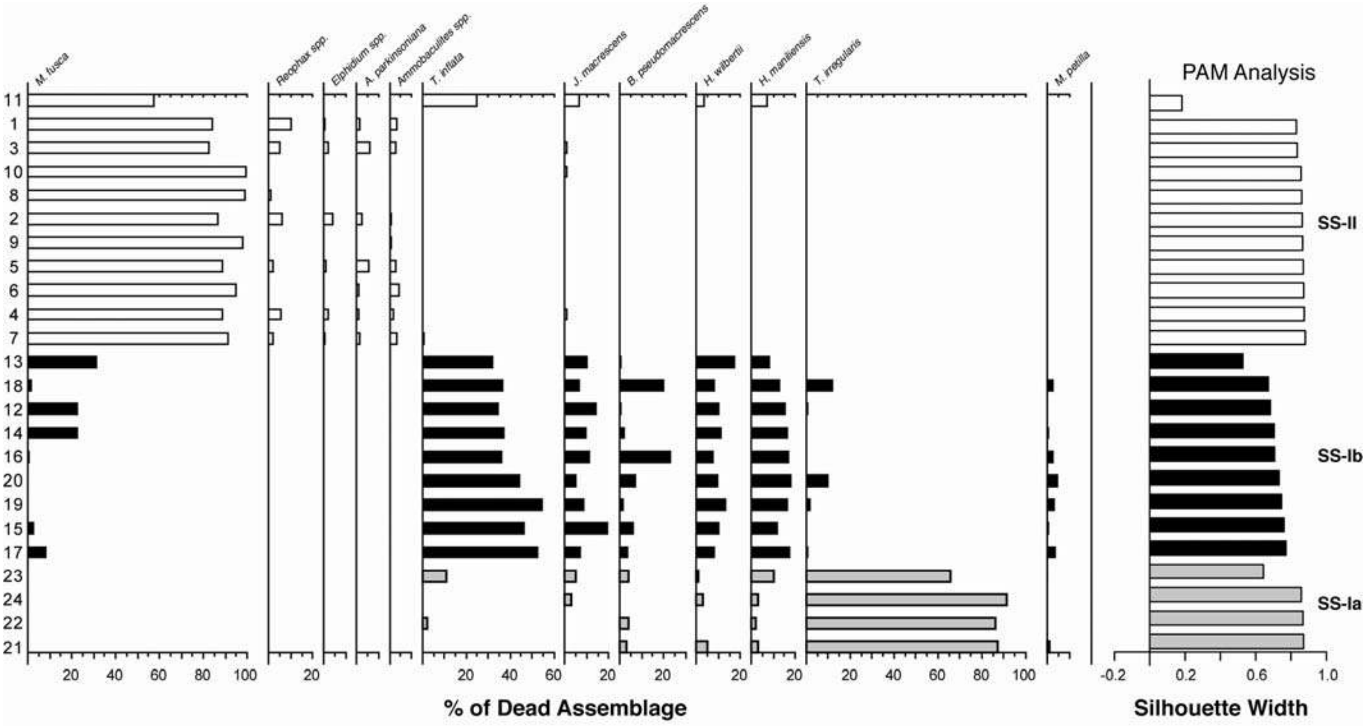

Figure 3

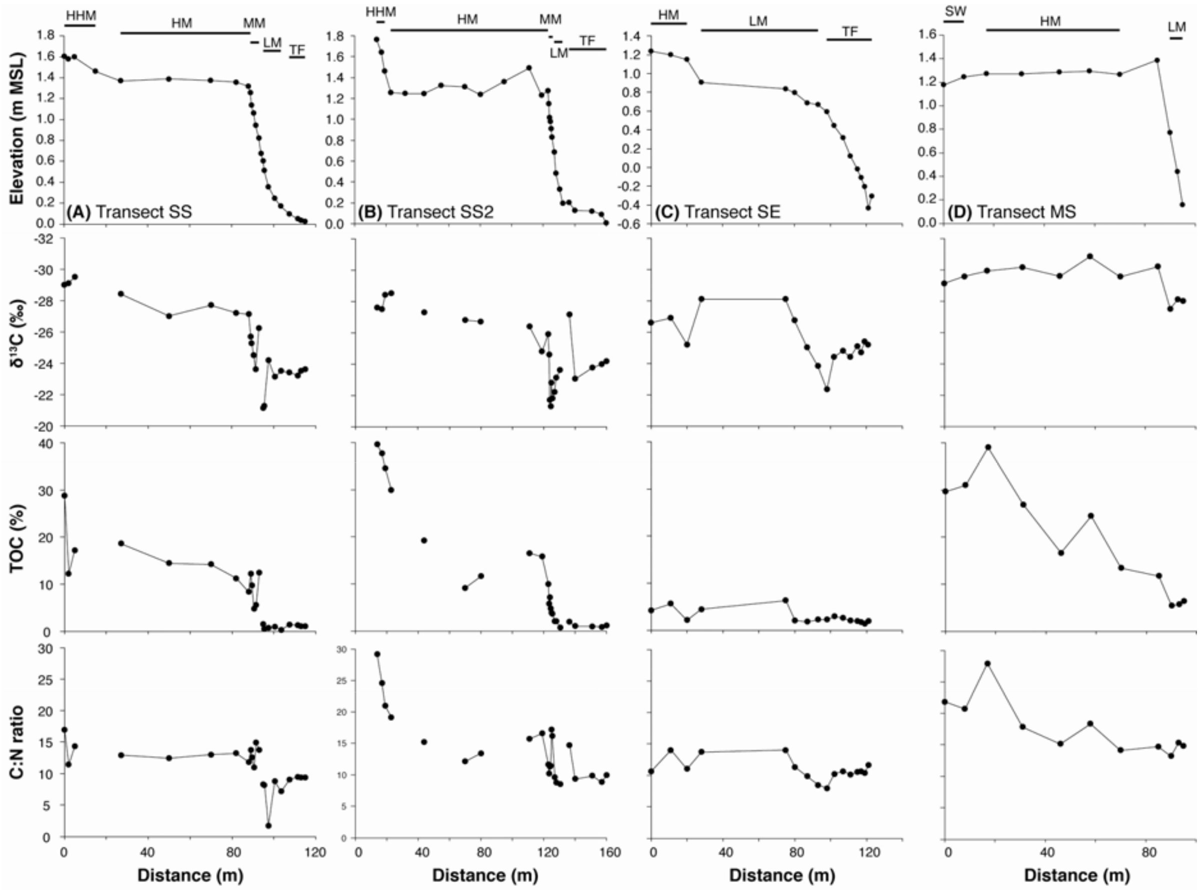
HHM
HM
MM
LM
TF
SW
Elevation (m MSL)
(A) Transect SS
(B) Transect SS2
(C) Transect SE
(D) Transect MS
δ13C (‰)
TOC (%)
C:N ratio
Distance (m)

Figure 4

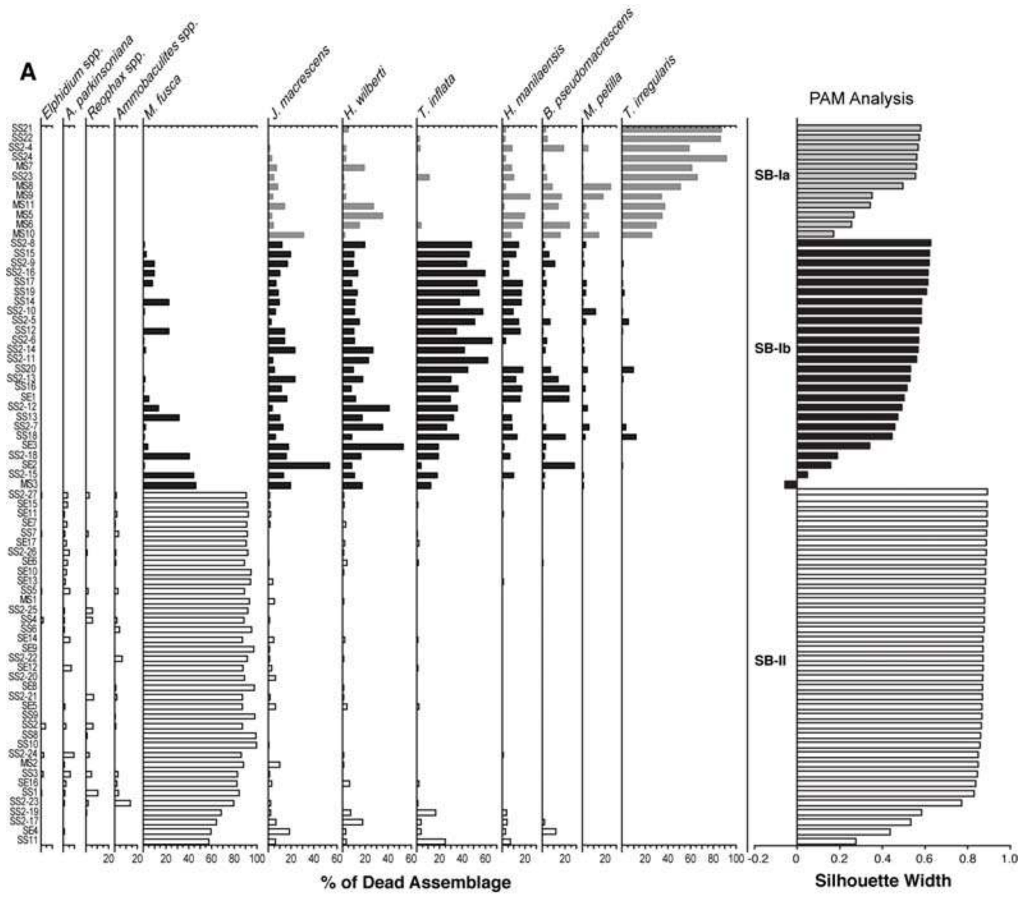
A
Elphidium spp.
A. parkinsoniana
Reophax spp.
Ammobaculites spp.
M. fusca
J. macrescens
H. wilberti
T. inflata
H. manilaensis
B. pseudomacrescens
M. petila
T. irregularis
PAM Analysis
SB-Ia
SB-Ib
SB-II
% of Dead Assemblage
Silhouette Width

Figure 5

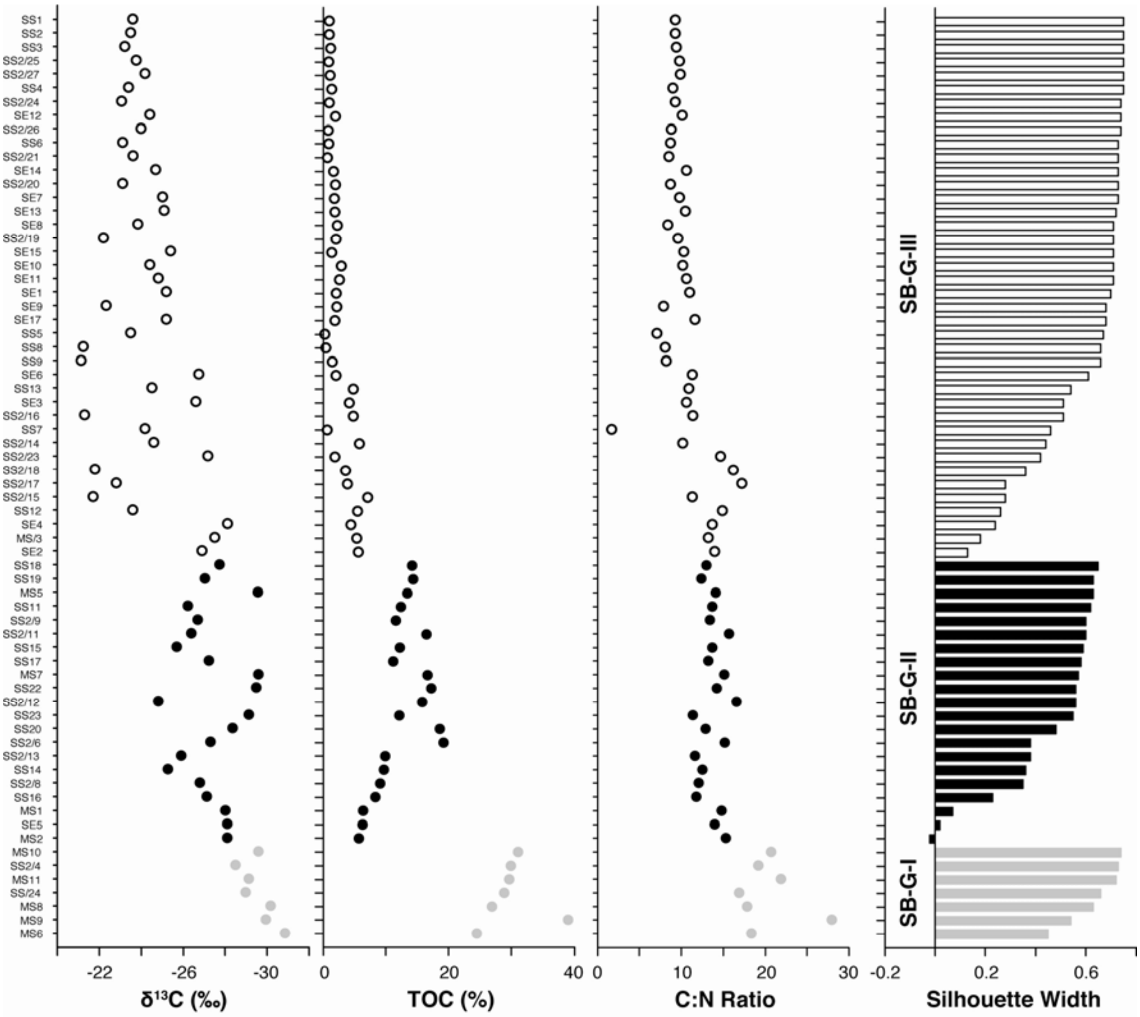
SS1
SS2
SS3
SS2/25
SS2/27
SS4
SS2/24
SE12
SS2/26
SS6
SS2/21
SE14
SS2/20
SE7
SE13
SE8
SS2/19
SE15
SE10
SE11
SE1
SE9
SE17
SS5
SS8
SS9
SE6
SS13
SE3
SS2/16
SS7
SS2/14
SS2/23
SS2/18
SS2/17
SS2/15
SS12
SE4
MS/3
SE2
SS18
SS19
MS5
SS11
SS2/9
SS2/11
SS15
SS17
MS7
SS22
SS2/12
SS23
SS20
SS2/6
SS2/13
SS14
SS2/8
SS16
MS1
SE5
MS2
MS10
SS2/4
MS11
SS/24
MS8
MS9
MS6
-22
-26
-30
δ13C (‰)
0
20
40
TOC (%)
0
10
20
30
C:N Ratio
-0.2
0.2
0.6
Silhouette Width
SB-G-III
SB-G-II
SB-G-I

Figure 6

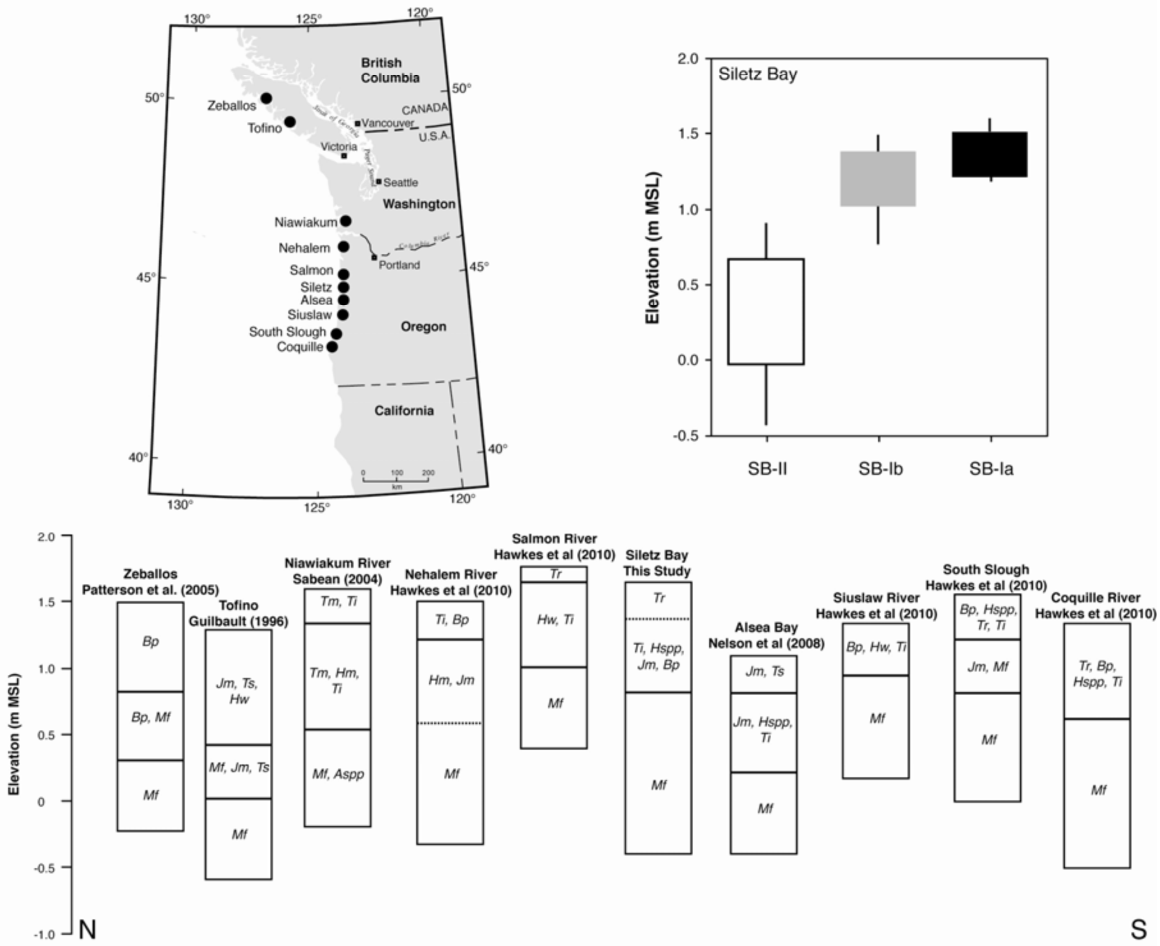
British Columbia
Zeballos
Tofino
Vancouver
CANADA
U.S.A.
Victoria
Seattle
Washington
Niawiakum
Nehalem
Portland
Salmon
Siletz
Alsea
Siuslaw
South Slough
Coquille
Oregon
California
130°
125°
120°
50°
45°
40°
Siletz Bay
Elevation (m MSL)
SB-II
SB-Ib
SB-Ia
Zeballos Patterson et al. (2005)
Tofino Guilbault (1996)
Niawiakum River Sabean (2004)
Nehalem River Hawkes et al (2010)
Salmon River Hawkes et al (2010)
Siletz Bay This Study
Alsea Bay Nelson et al (2008)
Siuslaw River Hawkes et al (2010)
South Slough Hawkes et al (2010)
Coquille River Hawkes et al (2010)
Bp
Bp, Mf
Mf
Jm, Ts, Hw
Mf, Jm, Ts
Tm, Ti
Tm, Hm, Ti
Mf, Aspp
Ti, Bp
Hm, Jm
Tr
Hw, Ti
Ti, Hspp, Jm, Bp
Jm, Ts
Jm, Hspp, Ti
Bp, Hw, Ti
Bp, Hspp, Tr, Ti
Jm, Mf
Tr, Bp, Hspp, Ti
N
S

Figure 7

Published in Paleo3, (2013) 377,13-27

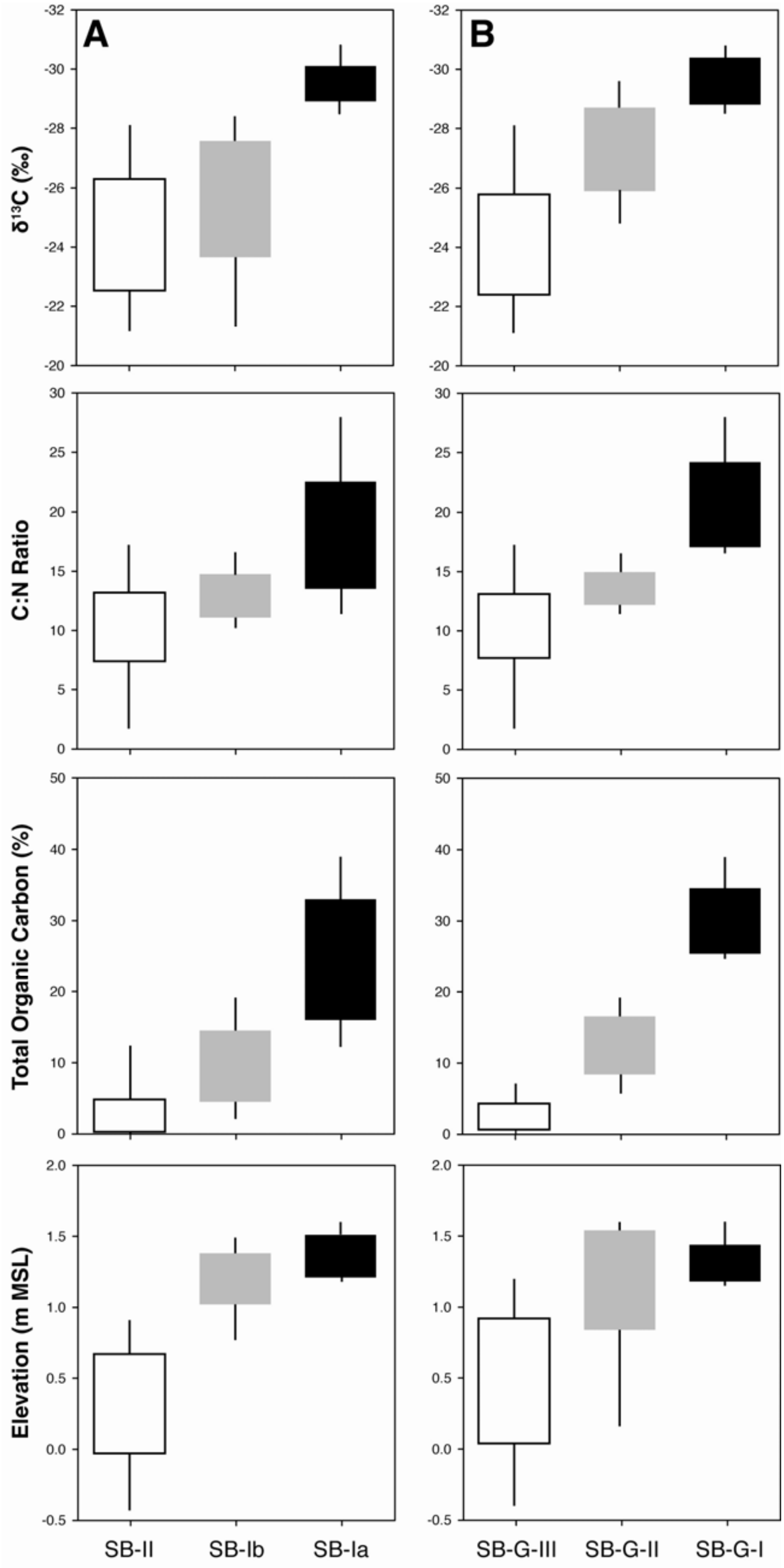

1123 Figure 8

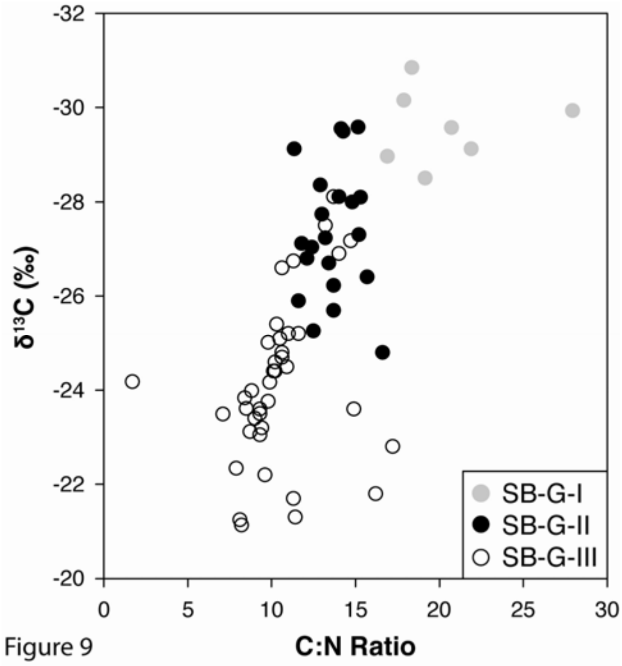
δ13C (‰)
C:N Ratio
SB-G-I
SB-G-II
SB-G-III
-32
-30
-28
-26
-24
-22
-20
0
5
10
15
20
25
30

Figure 9

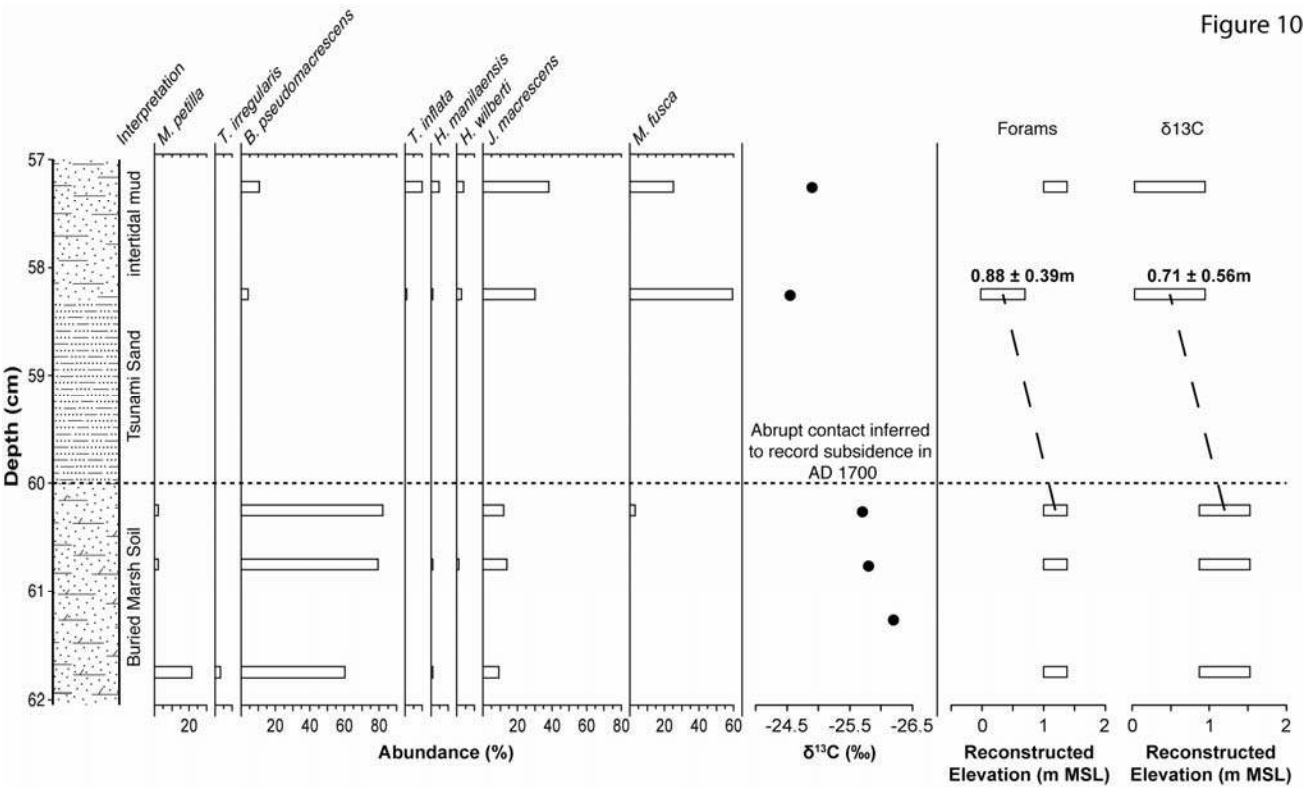
Figure 10
Interpretation
M. petilla
T. irregularis
B. pseudomacrescens
T. inflata
H. manilaensis
H. wilberti
J. macrescens
M. fusca
Forams
δ13C
Depth (cm)
57
58
59
60
61
62
intertidal mud
Tsunami Sand
Buried Marsh Soil
0.88 ± 0.39m
0.71 ± 0.56m
Abrupt contact inferred
to record subsidence in
AD 1700
20
20 40 60 80
20 40 60 80
20 40 60
Abundance (%)
-24.5 -25.5 -26.5
δ13C (‰)
0 1 2
Reconstructed
Elevation (m MSL)
0 1 2
Reconstructed
Elevation (m MSL)